A STUDY OF CRACK DETECTION MODEL

A Thesis

By

YANGMING SHI

Submitted to the Office of Graduate and Professional Studies of
Texas A&M University
in partial fulfillment of the requirements for the degree of

MASTER OF SCIENCE

Chair of Committee,	John M. Nichols
Committee Members,	Edelmiro F. Escamilla
	Douglas F. Wunneburger
Head of Department,	Joseph P. Horlen

December 2014

Major Subject: Construction Management

ABSTRACT

Pavement condition assessment is an important process in road maintenance and monitoring. However, current pavement condition assessment methods are time consuming and usually implemented manually. Pavement distress is becoming one of the biggest problems in road network systems. An efficient and effective detection method is needed to identify these pavement problems on the road. Additionally, crack detection is much more complicated than other infrastructure element detection. Current crack detection methods are complex and inefficient. Therefore, the purpose of this study is to create an efficient and effective crack detection model to identify cracks based on pavement images. This study uses a crack detection model with four components: image collection, image segmentation, pixel selection and statistical analysis. Image collection is a process of using a photogrammetry method to collect the data for the crack detection model. Then, the pavement image is transformed into a binary image during the image segmentation phase. Subsequently, the pixels in the binary image are selected in order to convert the photogrammetry data into statistical data. Finally, the statistical data will be analyzed using linear regression in order to determine whether the linear regression line represents an actual center line for the crack. This crack model is performed in a MATLAB prototype. The results indicate that this crack detection model can identify the center line of a crack accurately. Future work is suggested on controlling the data is piece of the linear regression algorithm.

DEDICATION

This thesis is dedicated to my mother, Li Yang, for her unconditional love and support throughout the course of my academic career and of my whole life. It is also dedicated to my friends, Yang Zhang, Xichen Wang and Jiale Xu, who always support me and help me in my life.

ACKNOWLEDGEMENTS

I would like to thank my committee chair, Dr. Nichols, and my committee members, Dr. Escamilla and Dr. Wunneburger, for their guidance and support throughout the course of this research.

Thanks also go to my friends and colleagues and the department faculty and staff for making my time at Texas A&M University a great experience. I also want to extend my gratitude to my friend Yang Zhang, who offered advice in programming.

Finally, thanks to my mother and father for their encouragement and support.

NOMENCLATURE

NAE	National Academy of Engineering
VPR	Visual Pattern Recognition
RGB	Red Green Blue
USDOT	U.S Department of Transportation

TABLE OF CONTENTS

Page

ABSTRACT ii

DEDICATION iii

ACKNOWLEDGEMENTS iv

NOMENCLATURE v

TABLE OF CONTENTS vi

LIST OF FIGURES viii

LIST OF TABLES xi

CHAPTER I INTRODUCTION 1

- Background 1
- Problem statement 2
- Research objective 2
- Hypothesis 2
- Study limitations 2
- Significance of this study 3

CHAPTER II LITERATURE REVIEW 4

- Introduction 4
- Definitions 5
- Visual pattern recognition model 5
- Current state of pothole detection 9
- Image segmentation for alligator crack 17
- Shadow noise in the image 19
- Median-filter algorithm 20
- Edge detection 22
- Standardization for camera images 23
- Factors that affect the quality of highways and roads 25

CHAPTER III METHODOLOGY 27

Introduction 27
Image collection 29
Image segmentation 43
Pixel selection 51
Statistical analysis 76

CHAPTER IV RESULTS 78

Introduction 78
The result of sample 2 78
The study limitation of sample 3 85

CHAPTER V CONCLUSION 86

REFERENCES 88

APPENDIX 92

LIST OF FIGURES

Page

Figure 1. 3D Modeling with VPR element models (After Brilakis et al, 2011) 7

Figure 2. VPR element models (After Brilakis et al, 2011).....9

Figure 3. Pothole detection model (After Koch and Brilakis, 2011) 11

Figure 4. Histogram shape-based thresholding algorithm (After Koch and Brilakis, 2011).....13

Figure 5. The result of image segmentation in pothole detection model (After Koch and Brilakis, 2011).....14

Figure 6. The original alligator crack image (After Li et al, 2014).....18

Figure 7. The alligator crack image after segmentation (After Li et al, 2014) 19

Figure 8. The picture analyzed by the median-filter algorithms (Maode et al, 2007).....21

Figure 9. Step edge and line edge (After Wang et al, 2012).....22

Figure 10. Pavement images corrupted by (a) a single source illumination with its histogram and (b) a multiple source illumination with its histogram (After Adu-Gyamfi et al, 2011).....24

Figure 11. Flow of pixel-by-pixel weighting (After Adu-Gyamfi et al, 2011).....25

Figure 12. Crack detection model 28

Figure 13. The location of picture collection 30

Figure 14. Picture collection 31

Figure 15. Picture collection equipment. 32

Figure 16. Photograph crack No.1 33

Figure 17. Photograph crack No.2 34

Figure 18. Photograph crack No.3 35

Figure 19. Photograph crack No.4 36

Figure 20. Photograph crack No.5 37
Figure 21. Photograph crack No.6 38
Figure 22. Photograph crack No.7 39
Figure 23. Photograph crack No.8 40
Figure 24. Photograph crack. No.9 41
Figure 25. Photograph crack No.10 42
Figure 26. The R_{sel} value of this picture is 10 45
Figure 27. The R_{sel} value of this picture is 20 46
Figure 28.The R_{sel} value of this picture is 50 47
Figure 29.The R_{sel} value of this picture is 100. 49
Figure 30.The R_{sel} value of this picture is 150. 50
Figure 31. Part of the result in the new matrix 53
Figure 32. The original location of each sample 55
Figure 33. The location of sample 1 in the matrix 56
Figure 34. The location of sample 1 in original image 57
Figure 35. The location of sample 2 in the matrix 58
Figure 36. The location of sample 2 in the original image 59
Figure 37. The location of sample 3 in the matrix 60
Figure 38. The location of sample 3 in the original image 61
Figure 39. The location of sample 4 in the matrix 62
Figure 40. The location of sample 4 in the original image 63
Figure 41. The location of sample 5 in the matrix 64
Figure 42. The location of sample 5 in the original image 65
Figure 43. The location of sample 6 in the matrix 66

Figure 44. The location of sample 6 in the original image 67
Figure 45. The location of sample 7 in the matrix 68
Figure 46. The location of sample 7 in the original image 69
Figure 47. The location of sample 8 in the matrix 70
Figure 48. The location of sample 8 in the original image 71
Figure 49. The location of sample 9 in the matrix 72
Figure 50. The location of sample 9 in the original image 73
Figure 51. The location of sample 10 in the matrix 74
Figure 52. The location of sample 10 in the original image 75
Figure 53. The draft result of crack detection for crack No.3 77
Figure 54. The result of sample 2 in Microsoft Excel 80
Figure 55. The plot of the linear regression 81
Figure 56. The result of residuals 82
Figure 57. Results of the analysis of variance 83
Figure 58. Fit Diagnostics for Row 84
Figure 59. The crack which could not be solved by this method 85

LIST OF TABLES

Page

Table 1. The programing code of MATLAB in the image segmentation process 92

Table 2. The program code of MATLAB in pixel selecting process 93

CHAPTER I

INTRODUCTION

BACKGROUND

The National Academy of Engineering (NAE) recently listed restoring and improving urban infrastructure as one of the "grand challenges of engineering in the 21st century" (Brilakis et al., 2011). At the same time, President Obama signed an $80 billion economic stimulus package to extend transportation infrastructure in the United States. Thus, infrastructure projects, especially highway projects, have developed quickly in recent years. Pavement condition assessment is an important process in road maintenance and monitoring. However, current pavement condition assessment methods are time consuming and are usually implemented manually. Based on a U.S Department of Transportation (USDOT) report, more than half of all major roads and highways in the United States are classified as being in fair or worse condition (Deason 1998). According to these assessment limitations, pavement distress is becoming one of the biggest problems in road network systems. An efficient and effective detection method is needed to identify these pavement problems on roads. Additionally, crack detection is much more complicated than other infrastructure element detection. Current crack detection methods are complex and inefficient. Therefore, the purpose of this study is to create an efficient and effective crack detection model to identify cracks based on pavement images.

PROBLEM STATEMENT

The problem statement is that the crack detection model used in this study could accurately identify the center line for a crack.

RESEARCH OBJECTIVE

The objective of the research is to use the crack detection model to identify the center line of cracks based on high resolution pictures.

HYPOTHESIS

The first hypothesis of this research is that all pixels can be accurately selected by the R (Red) value in the image segmentation phase. Different R values will be used in the RGB (Red Green Blue) selecting algorithm. However, it is hard to find an accurate selecting R value fit for image segmentation. Thus, the R value will be estimated by the picture result. In other words, the R value that could present a clear outline of the crack with less noise will be used in the following phase.

The second hypothesis is that the block can accurately count the pixel number. The edge of the crack can be accurately defined by the pixel selection and the continuous pixel pattern will be treated as a crack.

STUDY LIMITATIONS

The study limitations are:

- An accurately selected R value cannot be found in the image segmentation phase.
- “T” shape cracks cannot be detected using this method.
- The crack detection model is based on 2D level.

- Some pixel patterns which are cracks will be removed by the block selection and some independent small cracks cannot be identified using this method.
- Shadow noise and object influence are not considered in this study.

SIGNIFICANCE OF THIS STUDY

This study provides a new crack detection method to detect cracks based on high resolution pictures. This method is more efficient and effective than the traditional method. The crack detection model is a fundamental process for the Visual Pattern Recognition (VPR) model. This study also includes using an RGB selecting algorithm for image segmentation and using statistical analysis to detect the center line of a crack. This crack detection model could greatly reduce the computing cost for crack detection and develop an efficient pavement condition assessment method. It may save a great deal of time and money for evaluating pavement conditions of roads.

CHAPTER II

LITERATURE REVIEW

INTRODUCTION

In recent years, remote sensing technology has been widely used in industry. Visual Pattern Recognition (VPR) model technology is one of the most important technologies in remote sensing technology. These models have been employed in project monitoring and quality control. The Visual Pattern Recognition (VPR) model technology has been especially used in the field of infrastructure related areas to monitor the quality of infrastructure elements. Recently, VPR models of concrete columns, air pockets, exposed reinforcement and potholes have been created (Brilakis et al., 2011). However, the current study mainly focuses on the process of recognizing and detecting cracks in a Visual Pattern Recognition (VPR) model.

The literature review will be divided into three parts. The first part will define and introduce the framework of the Visual Pattern Recognition (VPR) model and current state of pothole detection. Additionally, the image segmentation process in the pothole detection model will be compared to the image segmentation process in the crack detection model. The 2D and 3D recognition process will also be introduced in this part. Finally, the method for improving crack detection reliability and efficiency will be summarized. The second part will illustrate some crack detection methods such as edge detection and median-filter algorithm. The third part will explore factors that may influence pavement quality.

DEFINITIONS

The definitions of interest in this work are:

- Rank-ordered adaptive median filter (RAMF): RAMF is based on a test for the presence of impulses in the center pixel itself, followed by a test for the presence of residual impulses in the median filter output (Hwang & Haddad, 1995).
- Visual Pattern Recognition: VPR can be used to model visual information as a sequence of image analysis steps that begins with the sensing of the 3D scene and concludes with a detailed description of the image (Brilakis et al., 2011).
- As-built model: As-built spatial modeling in civil infrastructure is the process of capturing the related infrastructure's spatial data and transforming it into an object-oriented representation (Brilakis et al., 2011).
- Photogrammetry is generalized as the technique of measuring 3D objects by taking multiple photographs from different perspectives (Mikhail et al., 2001).

VISUAL PATTERN RECOGNITION MODEL

In the review of literature, the Visual Pattern Recognition (VPR) model is a model that could automate the identification of infrastructure-related elements. In this research, cracks on the road are the objects of study. The general idea of the Visual Pattern Recognition (VPR) model will be used as part of the current work. In this study, the photogrammetry data will be translated into a statistical problem and the statistical results will reflect the photogrammetry realty. Brilakis et al. (2011) indicated that a framework for creating visual pattern recognition (VPR) models that automate the

recognition of infrastructure-related elements with machine vision and pattern recognition concepts based on their visual features is the first step in a larger agenda. This study uses a pixel selecting method to identity cracks on roads. This represents a fundamental step for the Visual Pattern Recognition (VPR) model of crack detection. Figure 1 shows 3D modeling with VPR element models. The relationship between VPR models and 3D models can be easily identified. The general idea of the VPR model is to collect infrastructure data by the remote sensing technology. Then, one must set up a model to recognize the objects of infrastructure elements. In addition, one matches these objects to the 3D points, which are collected by remote sensing in the cloud and then, sets up a 3D model. Goedert et al. (2005) maintained that there are two stages in as-built spatial modeling:

- Remote sensing/data collection and surface generation
- Object identification and extraction.

Figure 1 shows the framework of a Visual Pattern Recognition model.

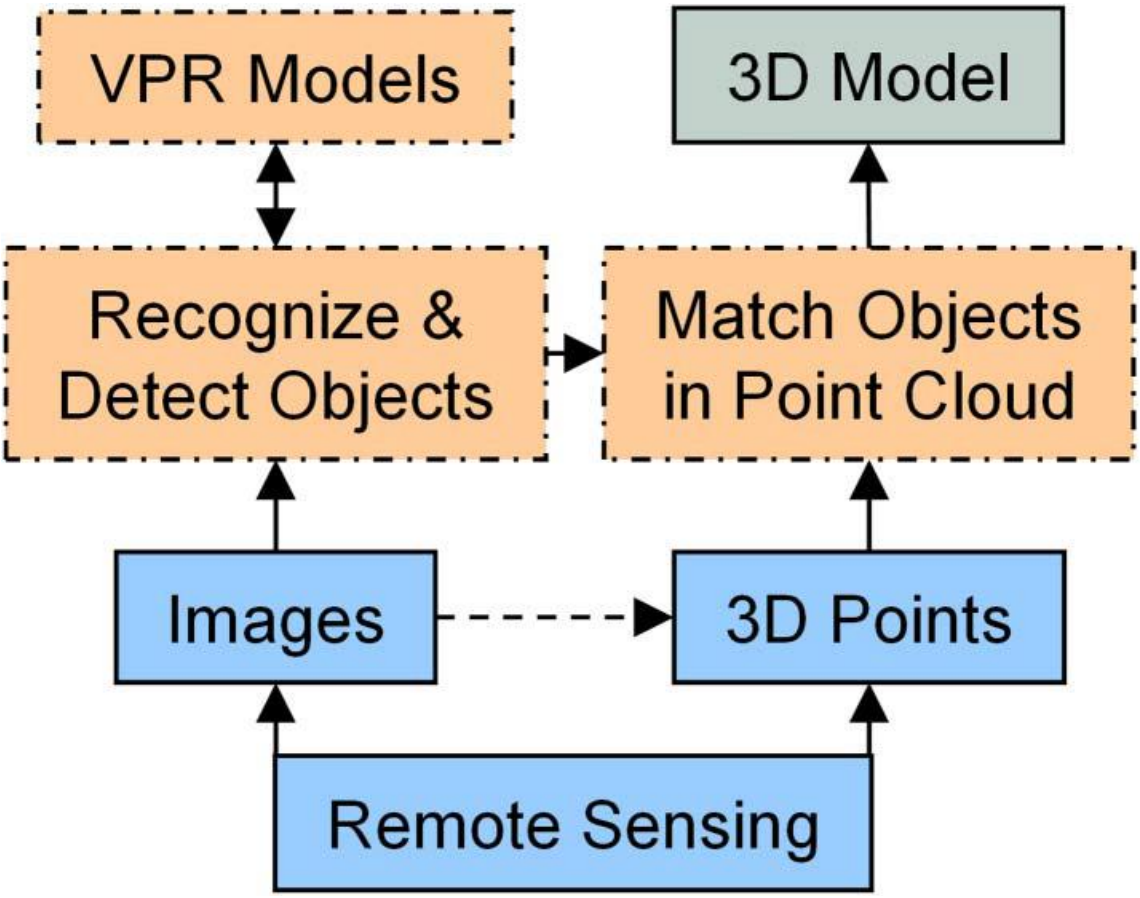

Figure 1. 3D modeling with VPR element models (After Brilakis et al, 2011)

For the data collection phase, there are numerous ways to collect the data such as high resolution camera and laser scanning. In this study, all the data are collected with a high resolution camera. This study uses three selection processes to convert photogrammetry data into statistical data and uses linear regression analysis to indicate the crack. This study mainly focuses on the process of recognizing and detecting objects. Figure 1 shows that the process from images to recognizing and detecting objects is fundamental for the whole Visual Pattern Recognition (VPR) model. Furthermore, this study also provides a new way to identify cracks based on high resolution pictures.

For the design phase, Figure 2 shows the Visual Pattern Recognition (VPR) element model. From this figure, it is easy to find that color, texture and structure are not the only features in a VPR element model; the spatial correlation of these features also plays a critical role. The features' 3D spatial correlations are also an important element in the model. In addition, Brilakis et al. (2011) indicated that there are three steps to create aVPR model:

- Identifying the distinctive characteristics of the specific infrastructure element;
- Numerically representing image analysis features with the identified distinctive characteristics;
- Spatially correlating features to form VPR models

In this study, these guidelines are used in detecting cracks on the road. The cracks on the road are all identified by the distinctive characteristics and all of these distinctive characteristics are converted into the numerical matrix.

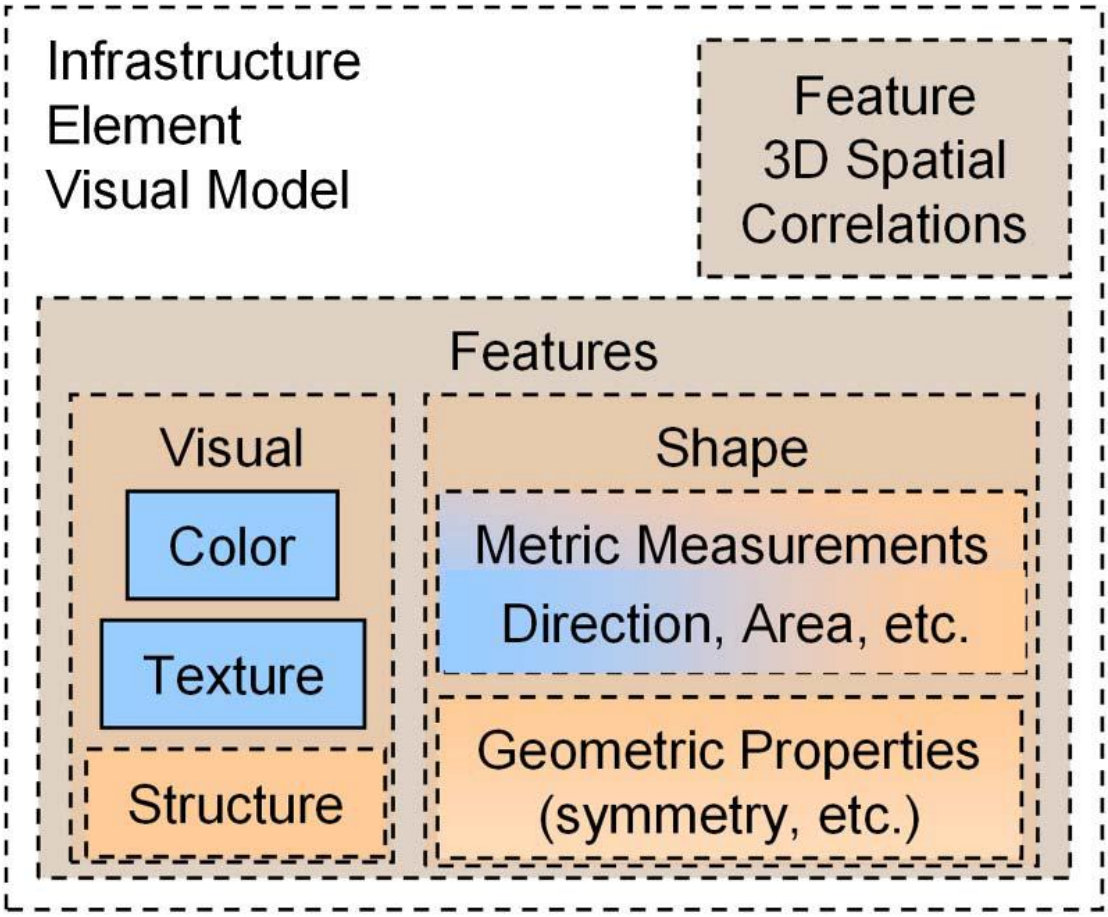

Figure 2. VPR element models (After Brilakis et al, 2011)

CURRENT STATE OF POTHOLE DETECTION

In this section, the current state of pothole detection practice will be introduced and compared to the crack detection method in this study. Pothole detection is quite similar to crack detection on roads. Both of them represent damage situations. In addition, both of them are caused by the failure of pavement. However, there are some differences between potholes and cracks. Most potholes are ellipses and are deeper than cracks. While most potholes exist individually cracks always exist as a group.

In their pothole detection study, Koch and Brilakis (2011) created a camera-based method for automated pothols detection based on asphalt pavement images:

- There are shadows (low-illuminated areas) that are darker than the surrounding healthy pavement;
- The shape is approximately an ellipse because of perspective;
- The texture of the material inside the pothole is grainier and coarser than the surrounding healthy pavement.

Based on the method mentioned above, it could be also used to identify cracks on the road. For the cracks in this study, the low-illuminated areas are darker than the surrounding areas, which means that the pixels' color in low-illuminated areas is darker than in the surrounding areas. In this study, the pictures are all converted into a 0 and 1 based matrix, with 0 representing white and 1 representing not-white. The pixels in low-illuminated areas are all 1 and the pixels in surrounding areas are all 0. Additionally, the texture of the material in potholes is coarser than the surrounding pavement; this concept could also be used for cracks. It means that the RGB value of pixels inside the crack is higher than for the surrounding pixels. All the principles mentioned above will be treated as the basic principles for the three step selection.

Koch and Brilakis (2011) created a three-step pothole detection model in recent research. The first step is image segmentation. The second step for this model is shape extraction. The third step for this method is texture extraction and comparison. Figure 3 shows the model for pothole detection.

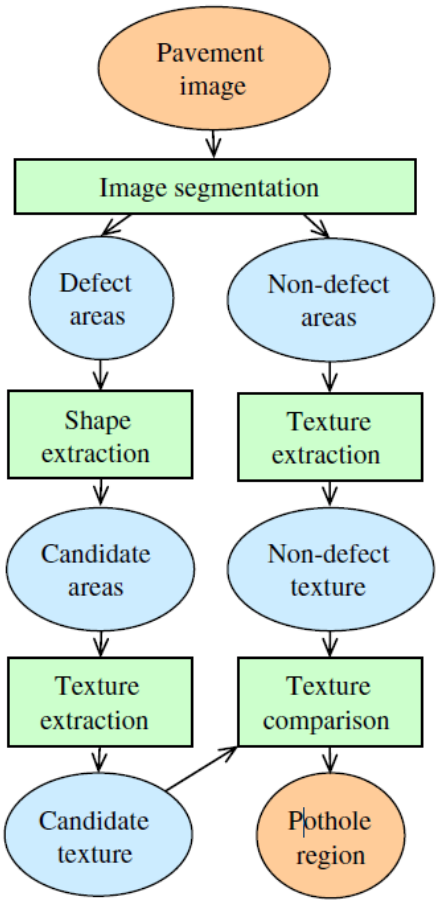

Figure 3. Pothole detection model (After Koch and Brilakis, 2011)

The shape extraction and texture extraction steps will be removed in the crack detection model in this study. Since most of the potholes are ellipse, the step of shape extraction is needed in the previous study to select the candidate areas. However, since most cracks are irregular curves, the areas of the cracks are so small that the shape extraction process is unnecessary in the crack detection model.

For the image segmentation process, Koch and Brilakis (2011) stated that in pavement surface images, color information, in particular RGB values, are not essential

when performing the segmentation process with regard to defect detection. However, the RGB value will be the primary threshold value in the first selection in this study. This is a big difference between the pothole detection model and the crack detection model. The purpose of this process is to transform the color images into gray-scale images. Additionally, Koch and Brilakis (2011) set up a 5 by 5 pixel median filter to reduce noise that is always produced by hardware during image or video capturing processes. This median filter method is used in the second step of the crack detection model in this study. Instead of a 5 by 5 filter, an 11 by 11 filter is used to remove the influence point or patterns.

Koch and Brilakis (2011) use a histogram shaped thresholding algorithm, which is based on the triangle algorithm presented in Zack et al. (1977)'s study. The purpose of this process is to separate the darker regions from the background for each picture. Furthermore, Koch and Brilakis (2011) indicated that in order to remove histogram peaks that might interfere with the subsequent method, a 1D median filter with order 5 is applied on the histogram. Then the threshold T is determined as the intensity value of a histogram point P_T = [T, h (T)], which has the maximum distance to a line l = [P0, P_{max}] that intersects the histogram's origin P_0 and the point P_{max} indicating maximum intensity. Figure 4 shows the histogram shape-based thresholding algorithm. Subsequently, based on the threshold T, Koch and Brilakis (2011) created Eq (1) to transform the enhanced image G_{enh} into a binary image B.

$$B(i,j) := \begin{cases} 1 \; if \; Genh\,(i,j) \leq T \\ 0 \; otherwise \end{cases} \qquad (1)$$

Figure 4 shows the histogram shape-based thresholding algorithm. The distance between P_T and line l is varied when P_T moves along the curve. The P_T indicates the maximum intensity in the picture.

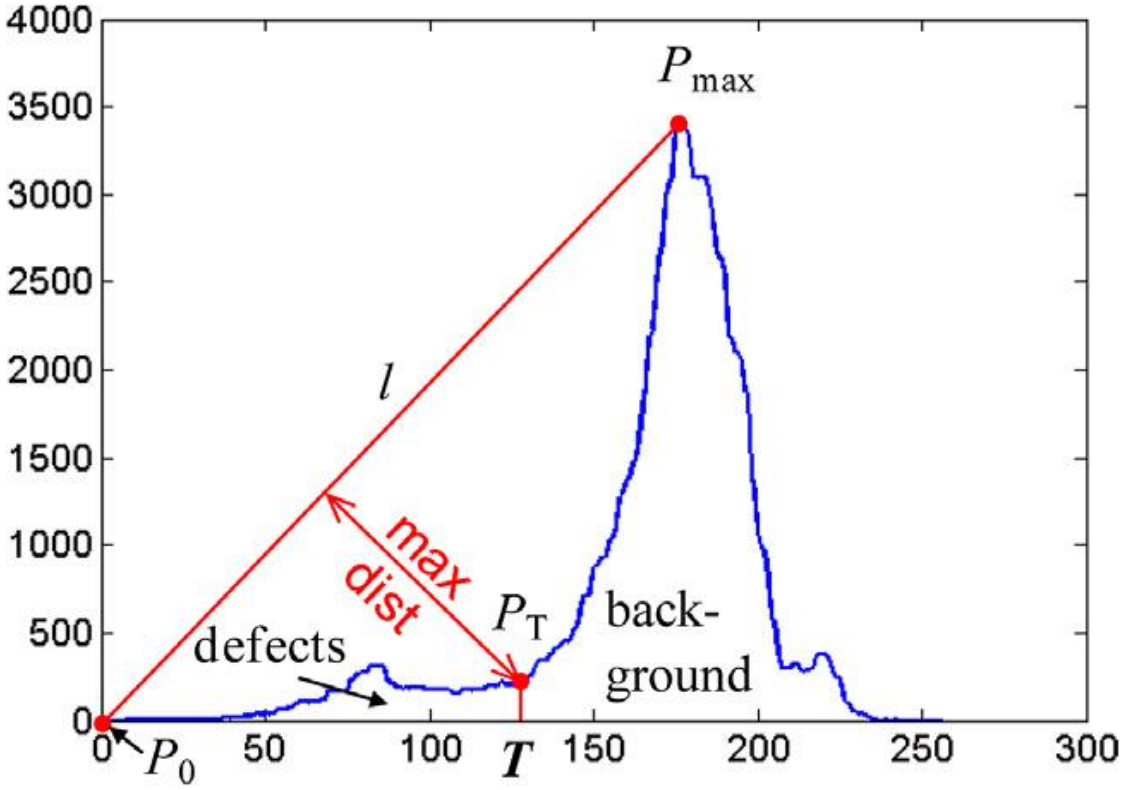

Figure 4. Histogram shape-based thresholding algorithm (After Koch and Brilakis, 2011)

Figure 5 shows the result of image segmentation in the pothole detection model. From Figure 5 (b), the pothole in the image is not completely identified. The reason for this problem may be the shadow in the pothole, which is a limitation of this algorithm. Figure 5 shows the result of image segmentation for two images of a pothole. Compared

to the image segmentation process in the pothole detection model, the image segmentation process in crack detection mainly focuses on the RGB value in the original image. The R (Red) value is selected as the primary threshold value in the image segmentation process. The range of R values is from 0 to 255. Different R values will be used to evaluate the results of binary images to find a threshold R value. Therefore, this method is similar to a histogram shape-based thresholding algorithm. The purpose of both methods is to convert the image into a binary image. The only difference between them is threshold value.

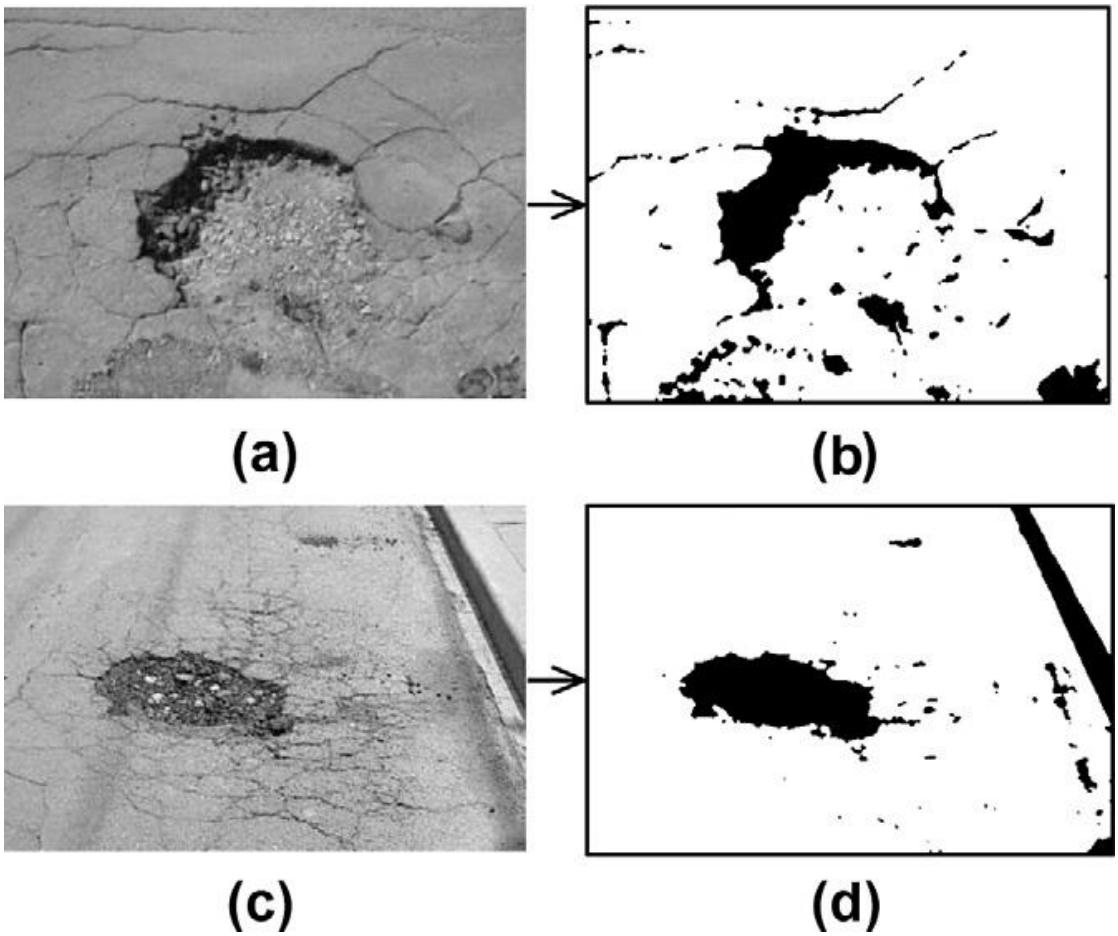

Figure 5. The result of image segmentation in pothole detection model (After Koch and Brilakis, 2011)

Furthermore, as most current pavement assessments are inefficient and costly, Jog et al. (2012) provided an inexpensive solution to detect potholes by using vision-based data for both 2D recognition and for 3D reconstruction. Similar to this, the videos in the current study were recorded by a high resolution camera. In this study, the number of potholes was counted by 2D recognition and the width and depth of the potholes and cracks were collected by 3D reconstruction. Jog et al. (2012) also stated that a pothole is recognized over a sequence of frames that facilitate calculating the total number of potholes. Additionally, representative healthy pavement texture is progressively generated over a sequence of video frames. However, crack detection is more complex than pothole detection. Although 2D recognition in his study was mainly focused on counting the number of potholes on the road, the 2D recognition analysis could not be used in this study.

Finally, the outcome of the sparse 3D reconstruction was improved using a dense reconstruction algorithm. However, some of the outcomes are the Poisson mesh model or the textured Poisson mesh model. For these models, the generated mesh model was used to measure the geometry of the potholes. The width and depth could be collected from these models. This research provides an efficient and inexpensive method to identify potholes and cracks not only by using pictures but also using video. The 3D recognition brings the vertical data of the crack into the analysis. At the same time, Torok et al. (2013) found that a 3D crack detection algorithm also provides the advantage of being able to operate on 3D mesh models regardless of their data collection source. Therefore, the 3D crack detection model was used in the present study.

The former camera-based pothole-detection method cannot identify the severity of potholes. The research presents a new method to improve detection reliability and to count potholes efficiently by updating a representative texture template for intact pavement regions and using a vision tracker to reduce computational effort. Compared with the method discussed above, there are two major advancements. First, texture signatures for the no distress, healthy areas of the pavement are incrementally updated to provide a more global and representative texture signature. Second, the detected pothole regions are tracked in subsequent frames for easy counting and reduction of computational effort (Koch et al. 2013). The new method increases the computational efficiency significantly. At the same time, the new method is more robust concerning abrupt surface and illumination changes. For the pothole track part, the pothole is tracked until it leaves the viewport and the pothole-detection algorithm is stopped at the same time. When multiple potholes are detected, the algorithm can run in parallel (Koch et al. 2013). The objective of this experiment was to count potholes, and the number of frames of the pothole regions was correctly tracked. The new method utilizes vision tracking to track detected potholes over a sequence of frames. This enables convenient pothole counting in pavement videos, avoiding inefficient redetection and matching in every frame, thus resulting in a significant processing time reduction. The proposed method assumes that only one pothole enters the viewport at a time. In cases of multiple potholes in the viewport, a combination of parallel detection and tracking is required while maintaining the computational effort at a minimum. Potholes always enter the viewport from the lower end of a frame and exit the viewport in the upper end of the

frame. Hence, in future work, the pothole detection algorithm will only be performed in the lower 1/3 of a video frame, whereas already detected potholes will be tracked in the whole video frame (Koch et al. 2013). In addition, once a pothole is detected, the corresponding region will not be considered in the detection procedure for the subsequent frame. By doing so, computational effort will not be compromised, and detection and tracking can still be conducted simultaneously. Moreover, multiple trackers can be instantiated in parallel if more than one pothole is detected.

IMAGE SEGMENTATION FOR ALLIGATOR CRACK

The paragraphs above illustrate the image segmentation process in a pothole detection model. The following paragraphs will introduce the image segmentation process for alligator crack, which is similar to the process for pothole detection.

Li et al. (2014) stated that the Otsu method finds the best threshold by maximizing the variance between foreground and background, and is widely used in image segmentation for many kinds of images because of its fast calculation. After an analysis using the Otsu method, the image may still have some influence points or patterns. However, in this study, the R (Red) value is treated as the primary threshold value in the image segmentation. Different R values will be used to transform the original image into a binary image. The binary image could be treated as a 0 and 1 matrix, with 0 representing white in the picture and 1 representing not-white. The purpose of image segmentation in this study is to find a threshold R value for the following phase. Li et al. (2014) used this method for an alligator crack. Figure 6 shows the original alligator crack image.

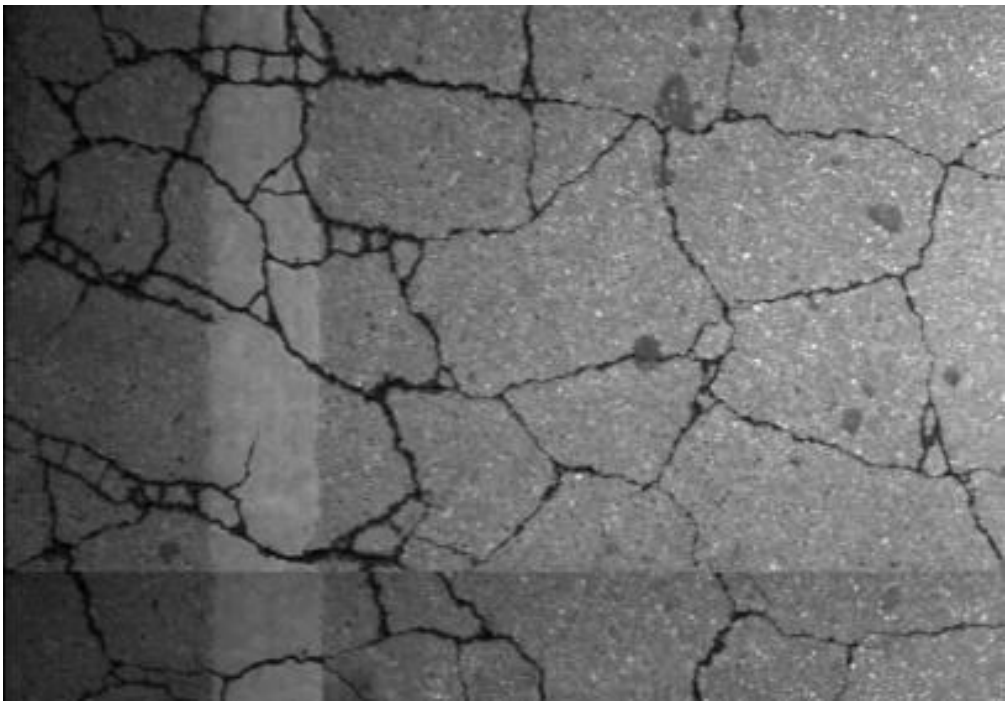

Figure 6. The original alligator crack image (After Li et al, 2014)

Figure 7 shows the alligator crack image after segmentation. For an alligator crack, the crack patterns are still quite clear after segmentation. Therefore, Li et al. (2014) concluded that the Otsu method provides good segmented crack images if the images have been properly preprocessed. In this study, the Otsu method also provides good segmented images in the first selection phase. The variance of shadow and objects on the road has little influence in this study.

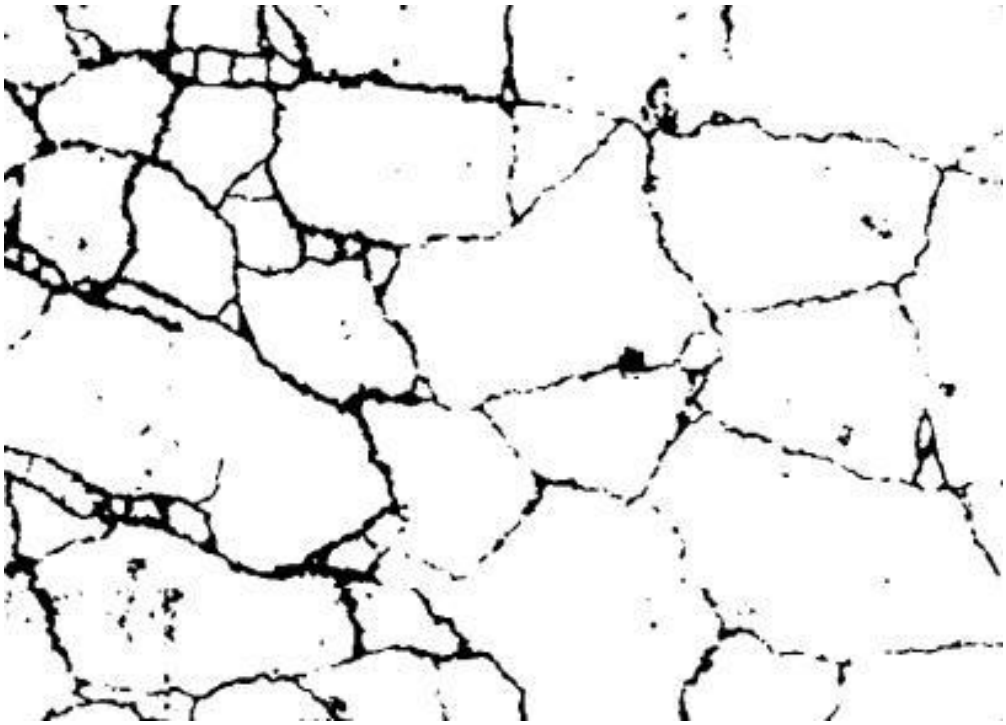

Figure 7. The alligator crack image after segmentation (After Li et al, 2014)

SHADOW NOISE IN THE IMAGE

As mentioned above, shadow influence in a picture is one of the biggest problems in crack detection. The computer system may define the shadow as cracks based on the color of the pixels. Thus, a shadow-removal algorithm is needed to remove the shadow in high resolution pictures.

Zou et al. (2011) introduced a new shadow removal method. Specifically texture-balanced luminance compensation method and Geodesic shadow-removal algorithm. Zou et al. (2011) applied a geodesic model to partition a shadow region into different levels so that the shadow strength within a single level is largely consistent. Then, they conducted a texture-balanced luminance compensation for each level to remove the

shadow. This method greatly reduced the shadow in the picture. It will help us remove variables in crack detection by selecting the crack by pixel color. However, the shadow removal process is not a main consideration in this study. When taking pictures for this study, the researcher tried to avoid the shadow problems that could occur.

MEDIAN-FILTER ALGORITHM

The median-filter algorithm will be introduced in this section. The method of median-filter algorithm is an important tool in the second selection of the crack detection model. The median-filter algorithm is used to remove noise in the image. According to the recent research, the median-filter algorithm and mean-filter algorithm methods are traditional ways to remove influence points or patterns. Maode et al. (2007) indicated that mean-filter usually fuzzes the edges of images, which makes images fuzzy in vision. In order to remove the influence points and patterns and not affect the edges of images, median-filter is preferred for the selection. The traditional median-filter is to set up a single template to filter noise. Figure 6 shows the result of a traditional median-filter. Figure 8 (a) is the original picture and Figure 8 (b) is the picture analyzed by the median-filter algorithm.

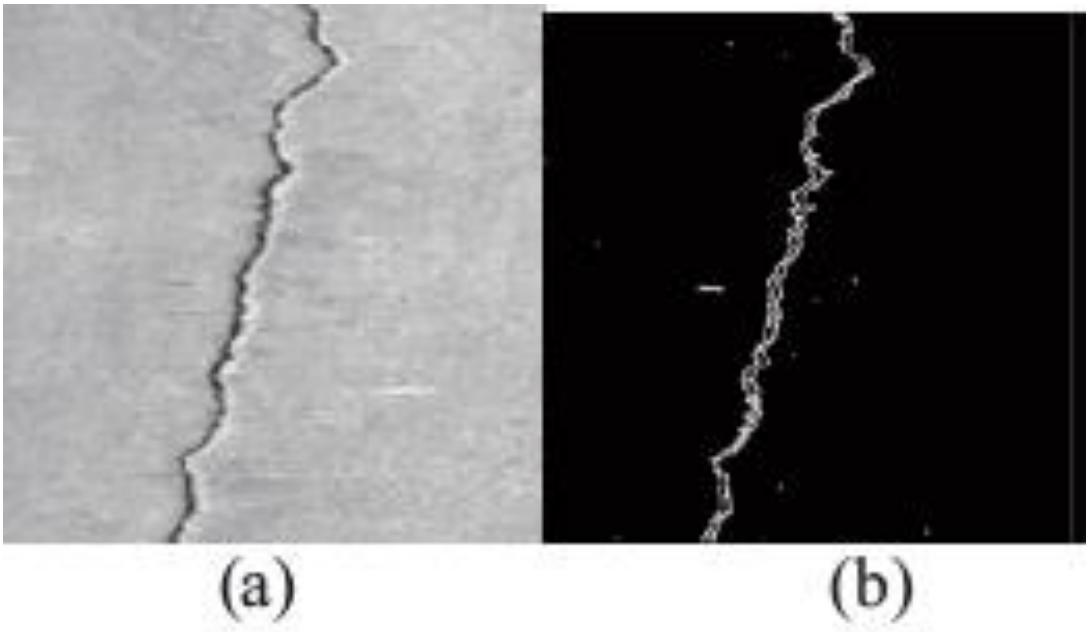

Figure 8. The picture analyzed by the median-filter algorithms (Maode et al, 2007)

After median-filter algorithm, there are still numerous influence points and patterns out of the crack. This study mainly focuses on the numbers in the crack to be statistically analyzed.

However, the median-filter algorithms also have some limitations. Wang (1999) indicated that when typical median filters are implemented uniformly across an image, they tend to modify both noise pixels and undisturbed good pixels. At the same time, Hwang and Haddad (1995) also indicated that the median filter performs quite well, but it falters when the probability of impulse noise occurrence becomes high. In this study, the median-filter algorithm is used in the second selection phase to remove influence points and patterns. Because of the method used in the first selection, the R value could

be adjusted in order to reduce the influence points and patterns. As such, the median-filter algorithm could greatly reduce the influence points and patterns in this study.

EDGE DETECTION

Liang and Sun (2010) indicated that edge detection is an alternative method for identifying and classifying pavement cracks for automated pavement management systems. Wang et al. (2012) indicated that two types of edges are usually contained in natural photographs: step edges and line edges. Wang et al. (2012) also illustrated that step edges emphasize region boundaries, whereas line edges are located within the narrow regions. Figure 9 shows both step edges and line edges. In this study, both have step edges and line edges. In order to detect these two types of edges, a Sobel Edge detector and Canny Edge detector were widely used in the edge detection.

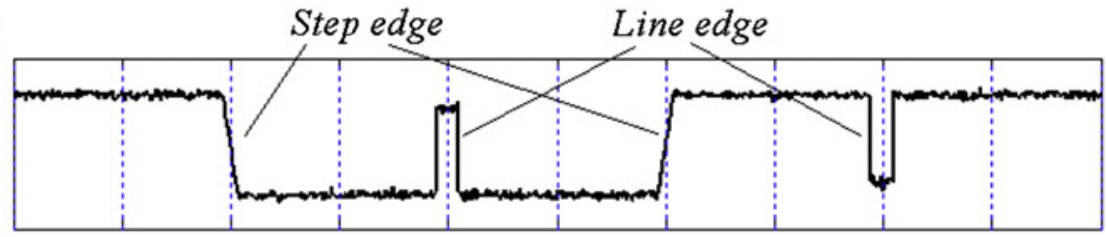

Figure 9. Step edge and line edge (After Wang et al, 2012)

Regarding the Sobel edge detector, Abdel-Qader et al. (2003) stated that it is known for its simplicity and speed, compared to other algorithms that are computationally complex, and is based on the spatial gradient algorithm. The problem of the Sobel edge detector is that it fails to define the edge when there are many influence

points or patterns in the picture. Thus, before using the Sobel edge detector, the picture should be analyzed to removing the influence points or patterns in order to detect the edges in the picture. Parker (2010) described the Sobel algorithm as the image data being convolved with a Sobel mask, resulting in first-order partial derivatives for the pixel in the middle of the mask. Compared to the Sobel edge detector, the Canny edge detector is more complicated. Abdel-Qader et al. (2003) indicated that the algorithm of the Canny edge detector is based on three parameters: σ, which is the standard deviation of the Gaussian mask, and t_{low} and t_{high} , which are used for thresholding to determine if a pixel belongs to an edge or not. However, Sobel mask methods are used in this study. In the second selection part in this study, a 10 x 10 size block is created to scan the matrix without repeat for not only minimizing the influence of the influence points and patterns but also detecting the edges. The edge is defined as the boundary of 0 and not 0.

STANDARDIZATION FOR CAMERA IMAGES

Adu-Gyamfi et al. (2011) stated that for low-cost camera images, variations in the background are the result of the shadows of trees and objects on the sides of roads. It is true that shadows or objects may influence the results in this study. Therefore, it is critical to remove the shadows and objects. As mentioned above, all the pictures used in this study were taken in the same lighting condition to avoid shadow problems. The process of image standardization is a process to remove any illumination variations.

Adu-Gyamfi et al. (2011) also indicated that two types of illumination effects are addressed: single source and multiple sources. Figure 10 shows examples of images corrupted from a single source and a multisource. From Figure 10, Adu-Gyamfi et al.

(2011) stated that the single source has a very simple bimodal histogram compared with that of the multisource shown in Fig. 10(b), making its characterizing or modeling more straightforward than the multisource. In this study, the pictures are all corrupted from difference sources. However, the shadow problem is not the primary consideration in this study.

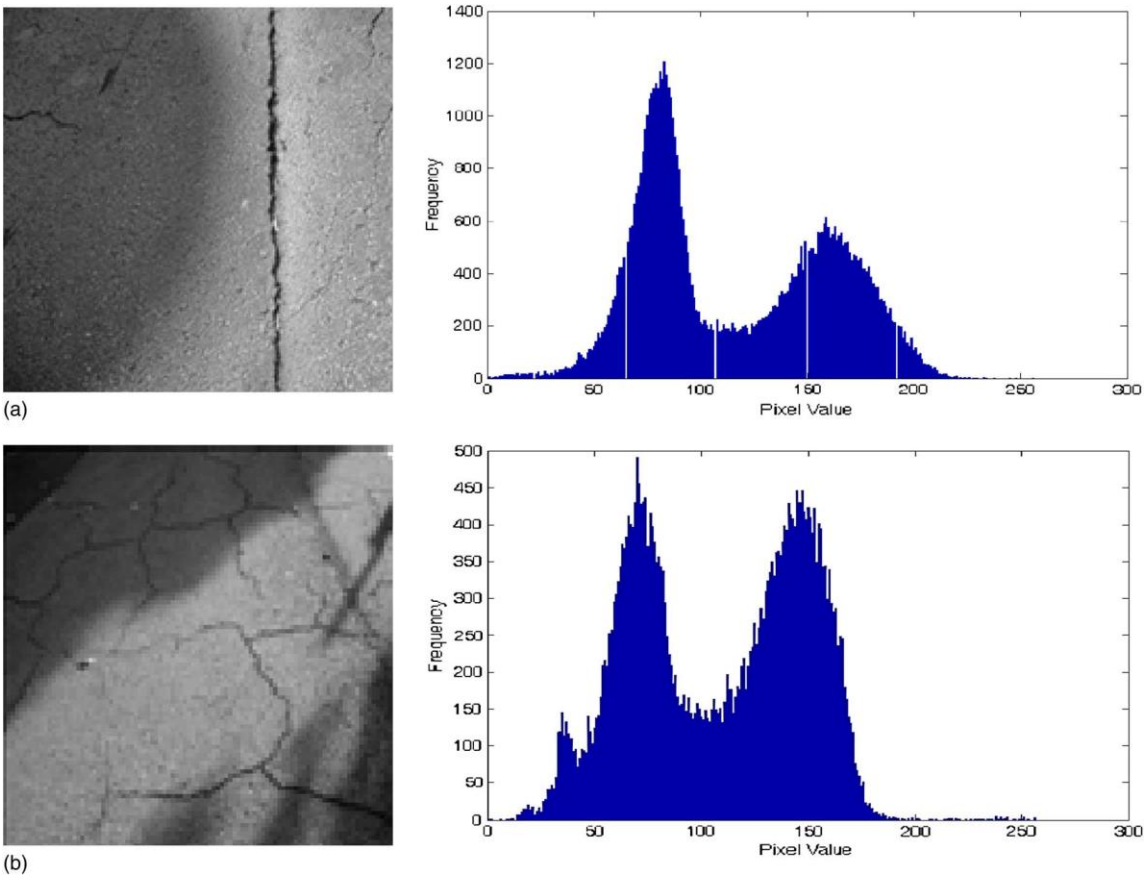

Figure 10. Pavement images corrupted by (a) a single source illumination with its histogram and (b) a multiple source illumination with its histogram (After Adu-Gyamfi et al, 2011)

Pixel by pixel weighting is an important process in this study's second selection part. Figure 11 shows the process of pixel by pixel weighting. The template will sum up the number in the box and move through this flow without repeat. This process can greatly remove influence points or patterns in images. At the same time, it can also standardize pictures.

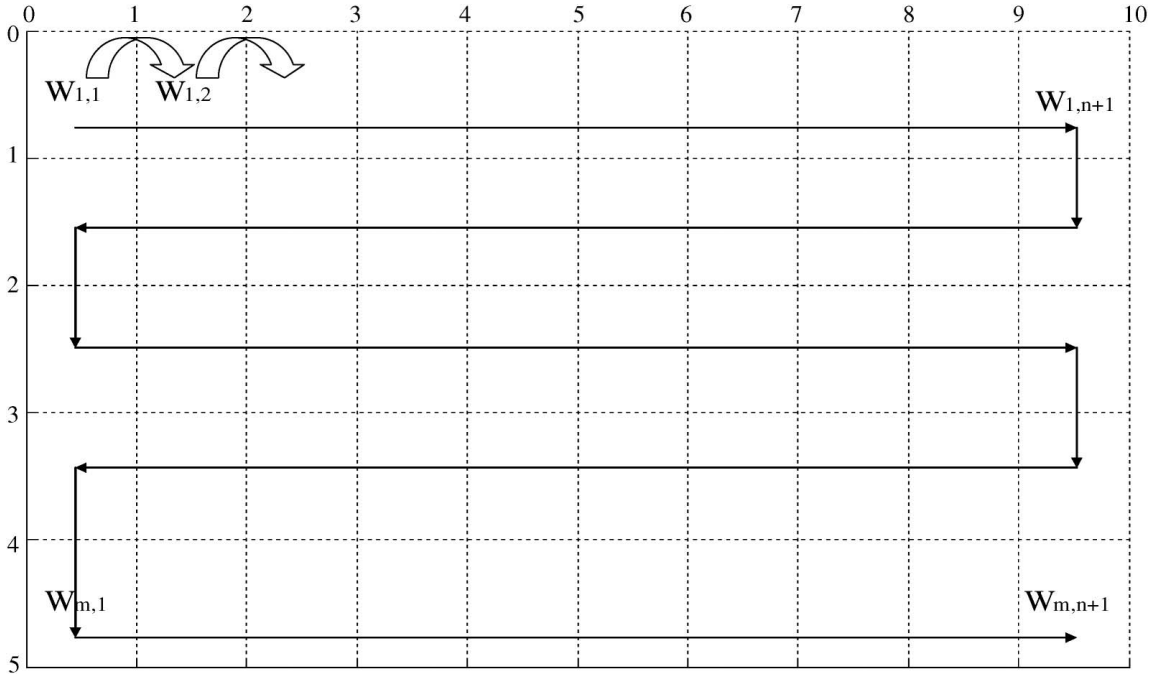

Figure 11. Flow of pixel-by-pixel weighting (After Adu-Gyamfi et al, 2011)

FACTORS THAT AFFECT THE QUALITY OF HIGHWAYS AND ROADS

From the literature review, there are 46 factors that may affect the quality of highways and roads. Five factor categories are selected as the factors related to US highway and road quality. The five categories developed by this process are as follows: (1) warranties and guarantees; (2) design standards; (3) bidding/contract award

procedures; (4) public private cooperation; and (5) research and development (Deason 1998). .Potholes and cracks in the highway are significant performance indicators of the quality of the highway. Potholes and cracks may be formed by poor construction or they may be formed due to other reasons.

According to Yu et al (2011), based on investigation data from over 60 km arterial highway in Jiangsu Province of asphalt pavement, transverse crack, longitudinal crack, patch and alligator cracking are typical stressors, which have significant impacts on pavement service quality. The conversion factor (k) of different distress factors is defined as an important factor for evaluation. The damage conversion factors (k) of different stressors are defined by the impact on service quality and the value reflects different impact severities. However, it is necessary to adjust k considering environmental and traffic conditions. The conversion factor k of the potholes ranged from 0.8 to 1 (Yu et al. 2011). The conversion factors of different types of distress and severity were adjusted in accordance with the impact of the distress on service quality and structural integrity.

CHAPTER III

METHODOLOGY

INTRODUCTION

The overall objective of this study is to create a comprehensive crack detection model to identify the existing crack base on a high resolution image. This study offers a fundamental process for the Visual Pattern Recognition (VPR) element model. This crack detection model is based on image segmentation, pixel selecting and statistical analysis. As mentioned in the literature review, Koch and Brilakis (2011) created a pothole detection model in their recent study. There are three components in pothole detection model which are image segmentation, shape extraction and texture comparison. The image segmentation process in this study is similar to the image segmentation in the pothole detection model. Due to geometric differences between cracks and potholes, the shape extraction and texture comparison process will not be discussed in this study.

As Koch and Brilakis (2011) indicated, a pothole includes one or more shadows that are darker than the surrounding area and the surface texture inside a pothole is much coarser and grainier than the surface texture of the surrounding material. Therefore, the fundamental principle of this crack detection model is that the color of pixels inside the crack is darker than the surrounding area. This principle will be mainly used in the crack detection process.

Figure 12 shows the crack detection model used in this study. This study starts with image collection to collect the pictures of the road.

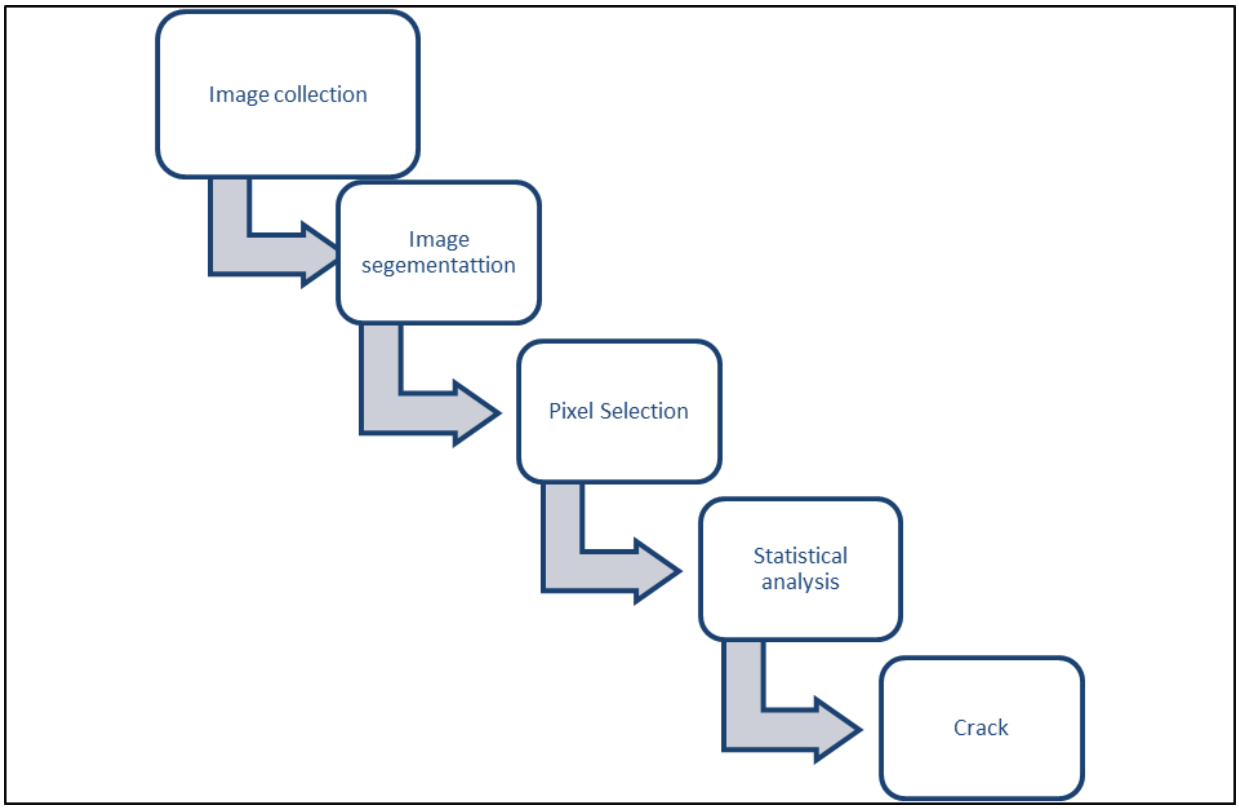

Figure 12. Crack detection model

All the images were collected under the same situation. Furthermore, this study uses image segmentation to transform the original image into a binary image. In this process, the image is converted into a 0 and 1 matrix. The R (Red) value is treated as primary threshold in this phase. Subsequently, the pixel selecting phase is used to sum up the pixels in the matrix and resize the matrix. Finally, the resized matrix will be statistically analyzed using linear regression. The result of the linear regression line is treated as the center line of the crack in the original image. The following paragraphs will illustrate the crack detection processes.

IMAGE COLLECTION

Image collection is the fundamental step for the crack detection model. The objective of this process is to collect the photogrammetry data for the crack detection model. Memon et al. (2005) stated that photogrammetry is a well-established approach and commonly used by architects and engineers to monitor highways. At the same time, Brilakis et al. (2011) also indicated that close-range photogrammetry is characterized by low equipment cost and fast on-site data acquisition at the expense of heavy user intervention to generate 3D surfaces from points. Thus, photogrammetry was found to be an effective and efficient way to collect images in this study. Additionally, this phase is an important process in the crack detection model since the quality of the image greatly influences the crack detection result. Based on the distinctive visual characteristics stated by Koch and Brilakis (2011), the surface texture inside a pothole is much coarser and grainier than the surface texture of the surrounding area. It means that the color inside the crack is darker than the surrounding areas. Thus, the images used in this study met the following principles:

- The crack could be clearly identified by the naked eye.
- The images were taken in the same lighting situation.
- The shadows and object influences were reduced.
- The color inside crack was darker than the surrounding areas.

Based on the principles above, the images were collected on the road in front of the College of Architecture at Texas A&M University. Figure 13 shows the location of the road. The red highlighted area in Figure 13 is the location of the road.

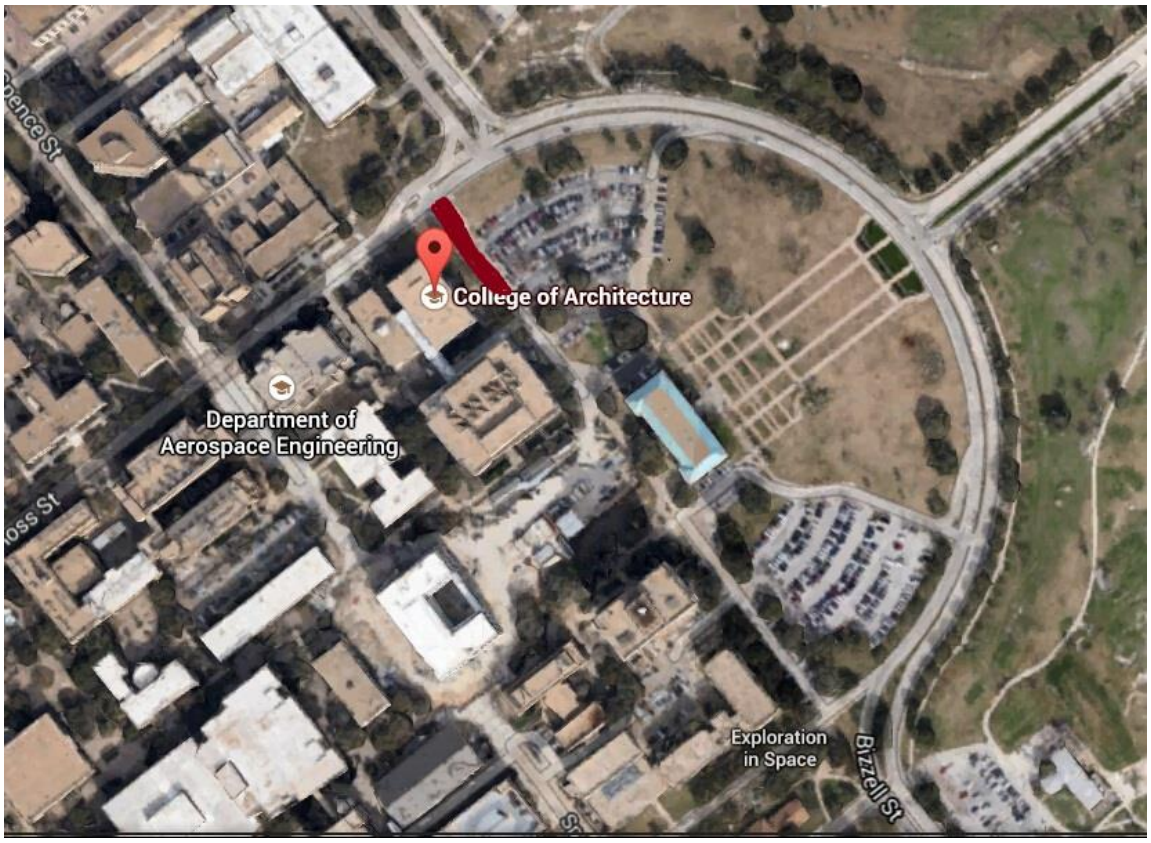

Figure 13. The location of picture collection

The reason for choosing this road is that it contains a myriad of cracks. Figure 14 shows the condition of the road. This road has been badly damaged for years and the cracks on the road can be clearly identified by the naked eye. Ten crack points on the road were randomly chosen. For each point, 50 pictures were taken with a high resolution camera.

Figure 14. Picture collection

The high resolution camera is a Canon EOS 60D. The lens of the camera is Canon EF 24-70 mm f/2.8. Figure 15 shows the camera that was used in this study. The

resolution of each picture was 5184 x 3456. The camera was fixed on the tripod in order to avoid any shaking problems during the shoot. In order to avoid shadow influences, each picture was taken under same lighting condition. Thus, the shadow influence is not a significant problem in this study.

Figure 15. Picture collection equipment.

At the same time, each picture was marked when the picture was taken. The following Figures 16 to 25 show the crack images collected by the researcher. The pictures are taken in the afternoon of January 24th in 2014. The weather of that day is clear. All the pictures are taken in the same lightening condition.

Figure 16 shows crack No.1. In this picture, two cracks are easily identified that meet at a “T” intersect.

Figure 16. Photograph crack No.1

Figure 17 shows crack No.2. In this picture, two cracks are easily identified meet at a “T” intersect.

Figure 17. Photograph crack No.2

Figure 18 shows crack No.3. In this picture, many cracks are easily identified. Crack No.3 has different types of crack such as “T” shape crack, leaner shape crack and alligator crack. In thus, Crack No.3 will be treated as the object in this study.

Figure 18. Photograph crack No.3

Figure 19 shows crack No.4. In this picture, many cracks are easily identified. Crack No.4 also has different types of crack such as “T” shape crack, leaner shape crack and alligator crack. However, the leaf influence may affect the result of crack detection. In thus, Crack No.4 will not be treated as object in this study.

Figure 19. Photograph crack No.4

Figure 20 shows crack No. 5. In this picture, many cracks are easily identified. Crack No.5 only has few cracks and the type of the crack is alligator crack.

Figure 20. Photograph crack No.5

Figure 21 shows crack No. 6. In this picture, three cracks are easily identified meet at two “T” intersect. In thus, there are two “T” shape crack in this image.

Figure 21. Photograph crack No.6

Figure 22 shows crack No. 7. In this picture, two cracks are easily identified meet at a “T” intersect.

Figure 22. Photograph crack No.7

Figure 23 shows crack No. 8. In this picture, two cracks are easily identified meet at a “T” intersect.

Figure 23. Photograph crack No.8

Figure 24 shows crack No. 9. Several cracks are easily identified in this picture. The type of the crack is alligator crack. The crack in the middle of the picture is hardly identify by naked eye.

Figure 24. Photograph crack. No.9

Figure 25 shows crack No.10. In this picture, two cracks are easily identified meet at a “T” intersect.

Figure 25. Photograph crack No.10

IMAGE SEGMENTATION

Image segmentation is the second step for the crack detection model. This step is the fundamental process for the crack detection model. The purpose of image segmentation is to transform the original image into a binary image. The binary image could be treated as a 0 and 1 matrix, with 0 representing white and 1 representing not-white. In order to achieve this objective, an RGB selecting algorithm is used in this phase. In Koch and Brilakis's (2011) study, they used a histogram shape-based thresholding algorithm, which is based on the triangle algorithm presented in Zack et al. (1977)'s study. The purpose of this process is to separate the darker regions from the background for each picture. Additionally, as mentioned in the literature review, Koch and Brilakis (2011) indicated that in pavement surface images, color information, in particular RGB values, are not essential when performing the segmentation process with regard to defect detection. However, compared to the algorithm used in the Koch and Brilakis (2011) study, the RGB selecting algorithm makes some improvements based on the histogram shape-based thresholding algorithm.

For the RGB (Red Green Blue) selecting algorithm, R (Red) value will be treated as the primary threshold value in image segmentation. The RGB values form the fundamental character in color information for the image, with a range from 0 to 255. When the red, green and blue values are all 255, the color of the pixel is white. When the red, green and blue are 0, the color of the pixel is black. The reason the R (Red) value is selected as the primary threshold value is that the R value is more efficient for representing the black-white strength for pixels. In the RGB selecting algorithm, the P

(i, j) represents pixels in the original image, B (i, j) represents the pixels in the binary image. If the R value of the pixel is smaller than the selecting R_{sel} value, the pixel will be defined as black, which is 1 in the binary image. Otherwise, the pixel will be defined as white, which is 0 in the binary image. Therefore, based on the threshold R_{sel} the original image will be transformed into a binary image using equation 2.

$$B(i,j) := \begin{cases} 1 \; if \; P\;(i,j) \leq \text{Rsel} \\ 0 \; otherwise \end{cases} \qquad (2)$$

This equation is similar to the equation used in the image segmentation in Koch and Brilakis's (2011) study. As mentioned in the literature review, Koch and Brilakis (2011) indicated that the threshold T is determined as the intensity value of a histogram point P_T = [T, h (T)], which has the maximum distance to a line l = [P0, P_{max}] that intersects the histogram's origin P_0 and the point P_{max} indicating maximum intensity. However, in the RGB selecting algorithm, the R_{sel} is the threshold value for the selection. The RGB selecting algorithm could save computing cost compared to the histogram shape-based thresholding algorithm. The RGB selecting algorithm mentioned in this paragraph is implemented in a MATLAB prototype, and the following paragraphs will discuss the results of the algorithm. Different R_{sel} values were used to evaluate the result of the binary image to find a threshold R_{sel} value.

In this study, crack No.3 (see Figure 18) is selected for analysis, because it has more cracks than other pictures. Because of this, crack No.3 significantly represents the problem of interest. Crack No.3 will be analyzed by different R_{sel} values in this study. Five R_{sel} values will be tested in this process. The general idea of the program is that if

the R value of a pixel is bigger than the R_{sel} value, the pixel will be defined as 0. At the same time, if the R value is smaller than the R_{sel} value, the pixel will be defined as 1.

Figure 26 shows the R_{sel} value of crack No.3 at 10. In this figure, because the R_{sel} value is 10, the R value of most pixels in this picture are greater than 10. In thus, most pixels are defined as white and it is hard to see the outline of the crack.

Figure 26. The R_{sel} value of this picture is 10

This R value is small, but the R value of most pixels will be bigger than the R_{sel} value. Therefore, most pixels will be definde as white when the computer is selecting pixels, making it difficult to see the outline of the crack in this picture. Therefore, the R_{sel} value of 10 is not significant for the picture to show the crack. As the R_{sel} value

increases, more and more pixels will be smaller than the R_{sel} value. Thus, more and more pixels will be defined as black in the selecting process. The outline of the crack can be more clearly seen when the R_{sel} value is increasing. Figure 27 and Figure 28 show R values of 20 and 50. Figure 27 shows the R_{sel} value of crack No.3 at 20. In this figure, the outline of the crack is more clearly seen than when the R_{sel} value is 10. Because the R_{sel} value is 20, more pixels in this picture are smaller than 20. Thus, the outline of the crack is clearer.

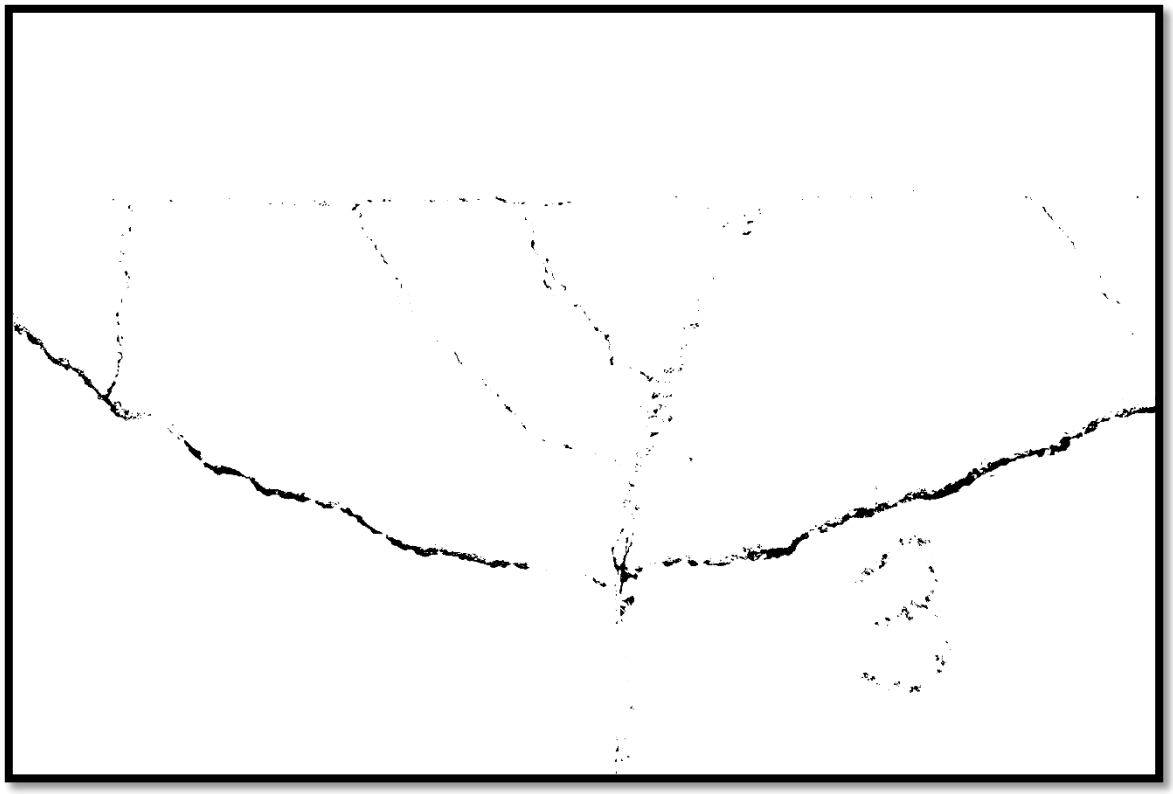

Figure 27. The R_{sel} value of this picture is 20

Figure 27 also shows that when the selecting R values increases, more pixels are selected and more pixels will be defined as black. The outline of the crack will be clearer than the picture in which R value is 10. When the R_{sel} value increases, more pixels will be selected during this process.

Figure 28 shows the R_{sel} value of crack No.3 at 50. In this figure, the outline of the crack can be totally seen. However, few influence points are seen out of the crack. This means than the R_{sel} value of 50 is greater than the suitable value. However, it is hard to find the accurate suitable value in this study using this selecting method. Therefore, the influence points will be removed in the second selection phase.

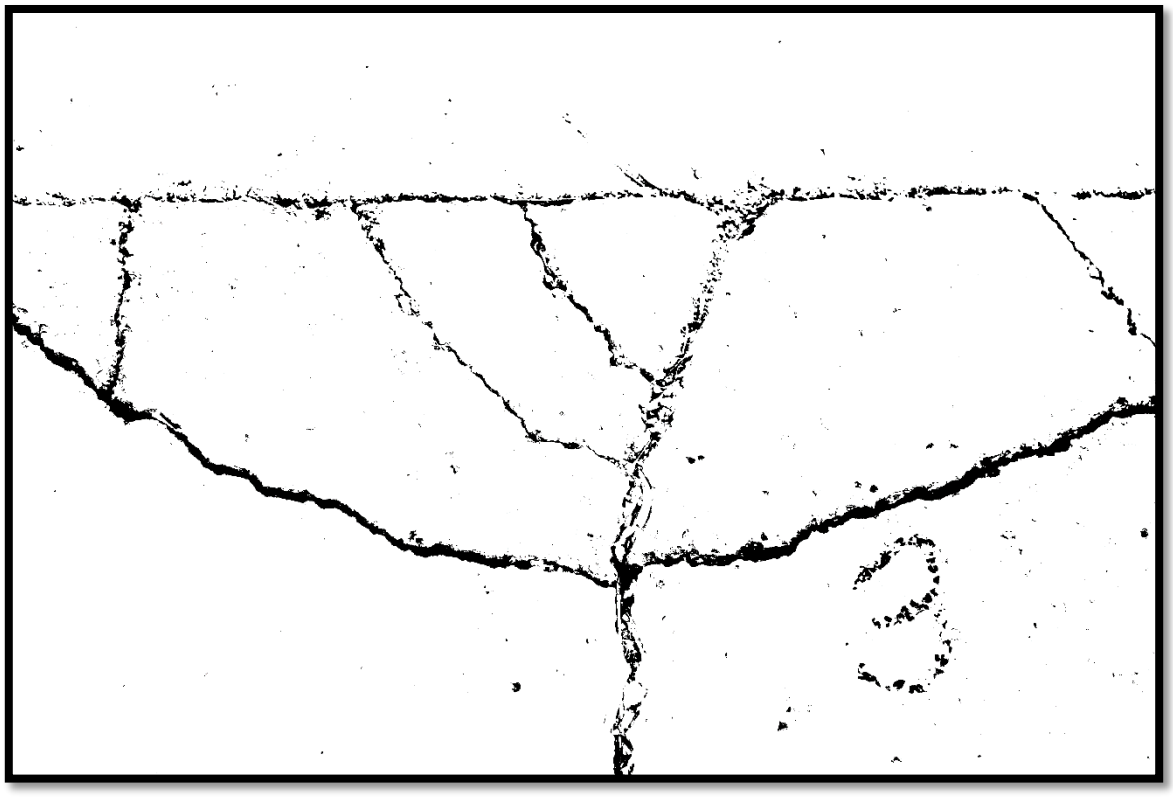

Figure 28.The R_{sel} value of this picture is 50

However, few influence points or patterns in the crack can be identified. Because of a selecting method flaw, it is hard to find an accurate R value that presents a totally clear crack without influence points or patterns. Therefore, in this study, an estimated R value was set up in this phase. This estimated R value clearly presents the outline of the crack. At the same time, few influence points or patterns exist in the picture. The second selection phase removes these influence points or patterns. However, when the R_{sel} value is greater than the estimated R value, more pixels will be smaller than the R_{sel} value. More and more pixels will be defined as black, even though the real color of the pixel is not black. Therefore, numerous influence points or patterns exist in the picture.

Figure 29 shows the R_{sel} value of crack No.3 at 100. In this figure, the outline of the crack can be seen. However, many influence points or patterns also exist in the image, and they would greatly increase the computing cost in the second selection. Therefore, the R value which is 100 is not a suitable R value. Figure 29 shows the R_{sel} value at 100. The outline of the crack can be seen in this picture. However, many influence points or patterns are also seen in this picture. These influence points or patterns greatly influence the computer to identify the crack. This also increases the computing cost in the second selection. A selecting R value of 100 cannot be used as the estimated value for the second selection.

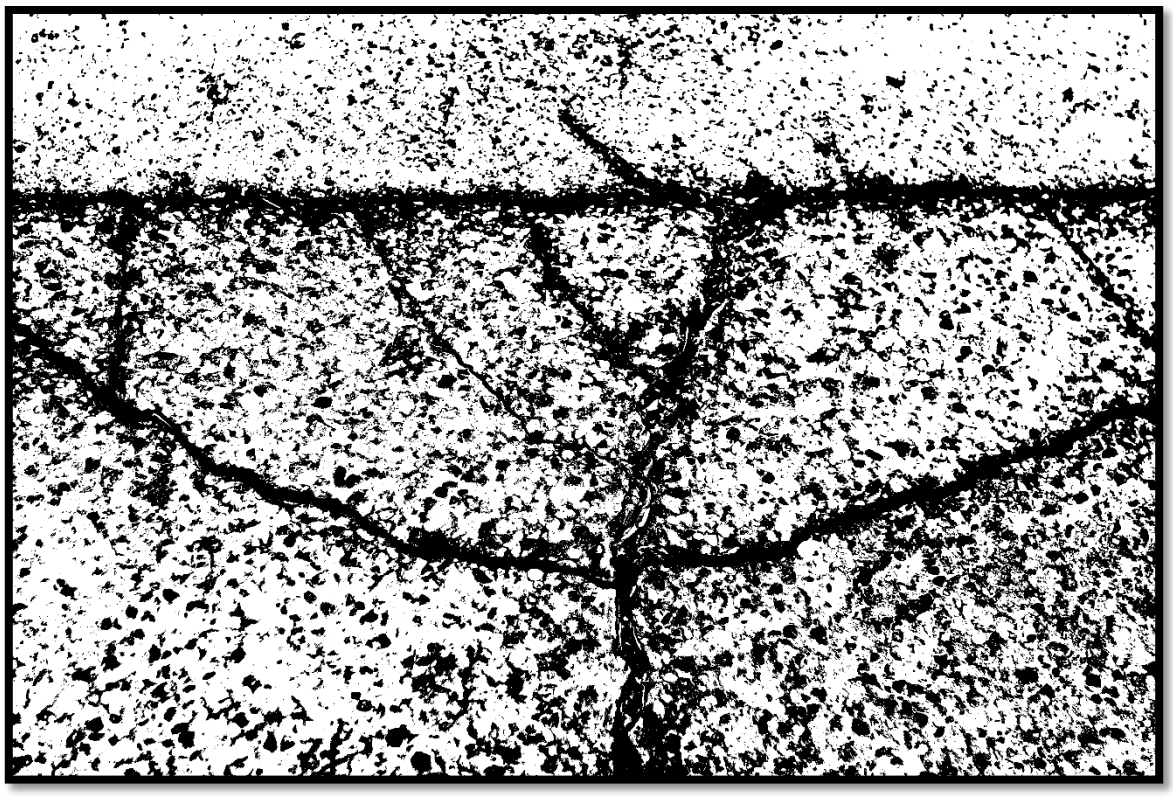

*Figure 29.*The R_{sel} value of this picture is 100.

Figure 30 shows the picture in which the R_{sel} value is 150. Due to most pixels being smaller than 150, an R_{sel} value which is 150 is too big for the selection. In fact, most of the pixels in crack No.3 could be defined as black in this selection. Thus, the result does not significantly show the crack outline in this picture. The outline of the crack can be hardly seen in this picture. Due to the R_{sel} value being much bigger than the estimated R value, most of the pixels in this picture are defined as black.

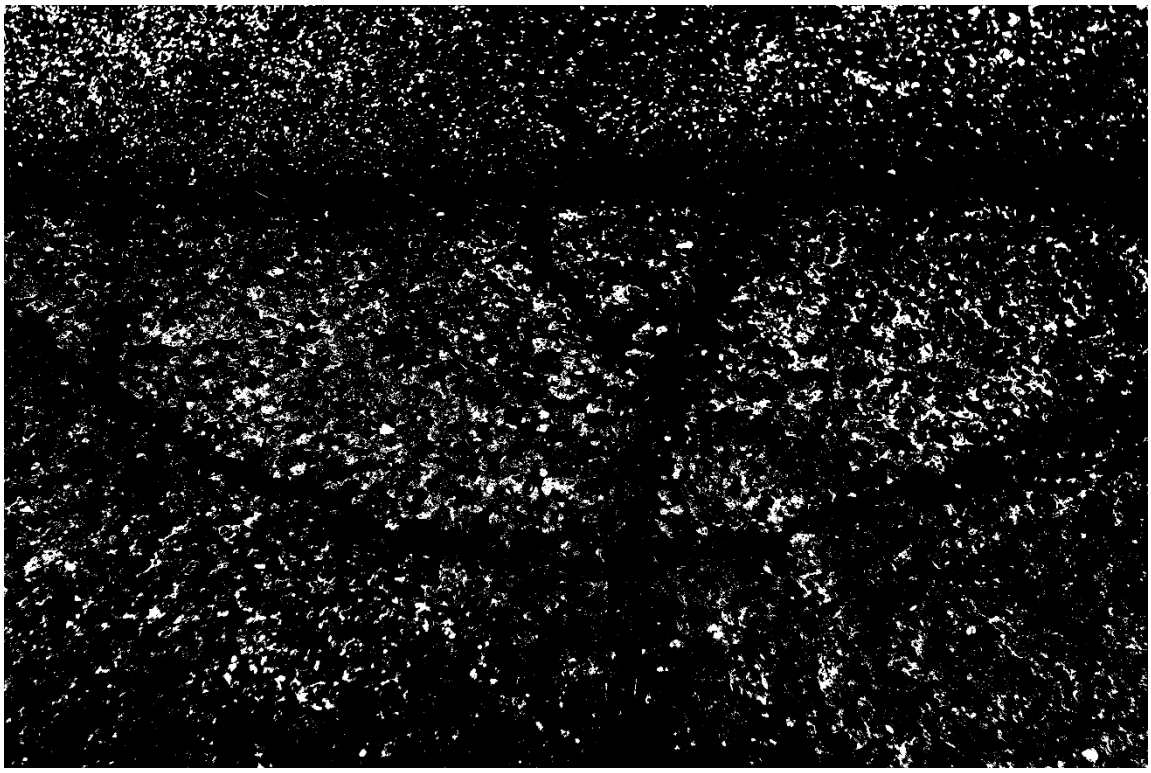

Figure 30.The R_{sel} value of this picture is 150.

Therefore, it is important to find an estimated R value that significantly shows the outline of the crack, but with fewer influence points or patterns. In Figure 29, the picture shows the outline of the crack. However, there are many influence points and patterns among the crack. The R_{sel} value, which is 100, is greater than the estimated R values. Additionally, the R_{sel} value should be smaller than 100 in order to remove influence points and patterns among the crack. Therefore, the estimated R value of the first selection should be located between 20 and 100. Finally, Figure 28 shows the R value at 50. In Figure 28, the crack outline can be clearly seen in the picture. At the same time, there are only a few influence points or patterns. As mentioned above, because of the selection method limitation,it is hard to find an accurate R value to present the outline of

the crack without any influence points or patterns. Therefore, in this study, an R_{sel} of 50 will be defined as the estimated R value in this study because it clearly presents the outline of the crack and the picture has fewer influence points or patterns. The analyzed picture will be used in the selection phase.

PIXEL SELECTION

Pixel selection is the third phase of the crack detection model. The objective of this phase is to transform the photography data into mathematical data. There are two functions for the pixel selecting method. The first function is to reduce the noise for the binary image. The second function is to identify the crack edge.

For the first function, the pixel selecting method used in this phase is similar to the median-filter algorithm. According to the literature review, the median-filter algorithm and mean-filter algorithm methods are traditional ways to remove influence points or patterns. Maode et al. (2007) indicated that mean-filter usually fuzzes the edges of images, which will make images appear fuzzy. In order to remove the influence points and patterns and not affect the edges of images, the median-filter is preferred for the selection. Similar to the traditional median-filter algorithm, the pixel selecting method is also set up on a single template to filter noise. The size of template or block in the pixel selecting method is 10 by 10. However, median-filter algorithms also have some limitations. Wang (1999) indicated that when typical median filters are implemented uniformly across the image, they tend to modify both noise pixels and undisturbed good pixels. At the same time, Hwang and Haddad (1995) also indicated that the median filter performs quite well, but it falters when the probability of impulse noise occurrence

becomes high. Therefore, the pixel selecting method used in this study is improved based on the idea of the median filter algorithm.

For the second function, the pixel selecting method is also used to detect the crack edge in the image. Edge detection is one of the biggest problems in crack detection, but it is critical for crack detection. The pixel selecting method can also help the computer to identify the edge of the crack in this phase. According to the literature review, Liang and Sun (2010) indicated that edge detection is an alternative method in the process for identifying and classifying pavement cracks for automated pavement management systems. Wang et al. (2012) indicated that there are two types of edges usually contained in natural photographs: step edges and line edges. Wang et al. (2012) also illustrated that step edges emphasize region boundaries, whereas line edges are located within the narrow regions. In this study, most of the crack edges are step edges.

Based on the two functions introduced above, the pixel selecting method will be presented in the following paragraphs. The pixel selecting method is based on the binary image created in the image segmentation. In this phase, a 10 by 10 template or block was created in the binary image. The binary image could be treated as a 5184 by 3456 matrix, consisting of 0s and 1s. The block scanned along the flow of the 5184 by 3456 matrix without repeat (see Figure 11). The pixels which were counted by the block were not calculated in the next calculation process. This process is called pixel by pixel weighting. During this process, the numbers in the block are summed up. For instance, the block size is 10 x 10. The total pixel number in this block is 100. The numbers in the block were summed up and transferred into a new number in the new matrix. In the end, the

old matrix, which is 5184x 3456, was converted into a 518 x 345 new matrix. Equation 3 shows the mathematic process. M (k, l) represents pixels in the new matrix.

$$M(k,l)=\sum_{i=10k+1}^{(10+1)k}\sum_{j=10l+1}^{(10+1)l}B(i,j) \qquad (3)$$

As mentioned above, the purpose of this selection is to remove the pixels or pixel patterns that are not cracks. At the same time, this pixel selection can help the computer identify the edge of the crack much easier than can the first matrix. Also, this pixel selection method does not affect the outline of cracks in the image. Figure 31 shows one part of the result for the new matrix.

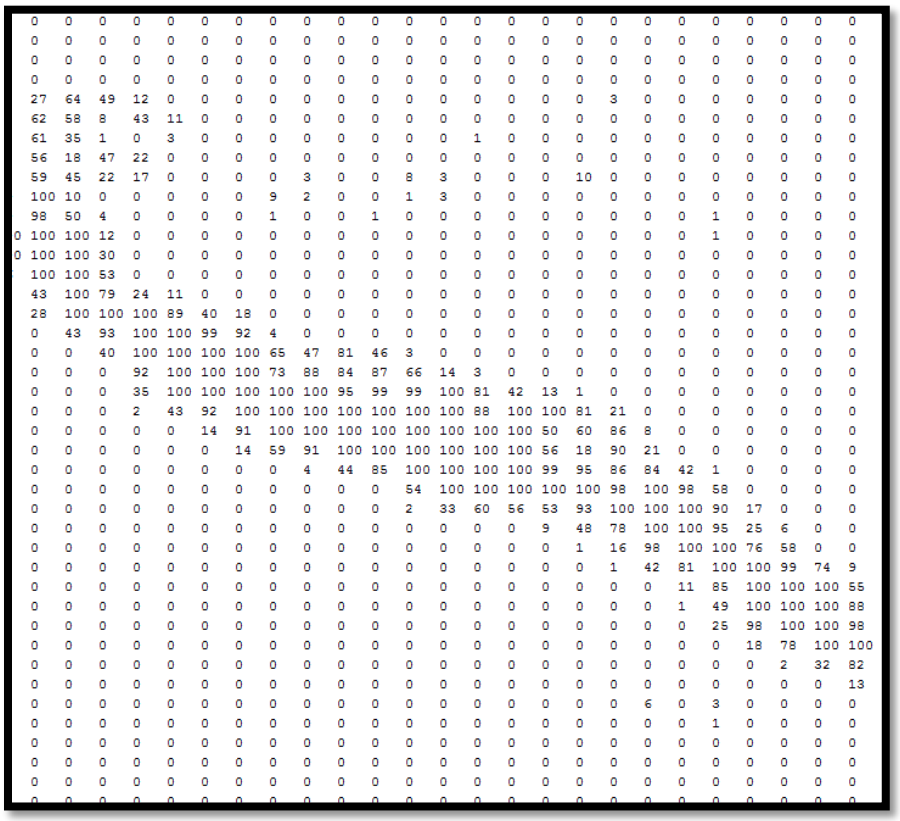

Figure 31. Part of the result in the new matrix

The coordinates in Figure 31 indicate the total number of 0 and 1 pixels in the binary image. Based on Figure 31, most of the influence points or patterns were removed by this pixel selecting method. However, some noise still existed in the new matrix. The number or number pattern which is surrounded by 0 means influence points or patterns. Continuous number pattern lines which are surrounded by 0s represent the crack in the original image. The edge of the crack can be easily detected by using this method. This new 518 x 345 new matrix will be used in the next phase to find the linear regression line among the number patterns.

Furthermore, as mentioned above, the purpose of the pixel selecting method is to transform the photography data into a mathematical data. It is necessary to indicate the original location of the crack which is a continuous number pattern line in the new matrix. In this phase, ten samples were randomly chosen in the new 518 by 345 matrix. The locations of each sample can be found in the original picture as shown in Figure 32. Each sample represents the cracks in the original image, which are easily identified by the human naked eye. The purpose of the pixel selecting method is to let the computer identify these number patterns in the new matrix as a crack. The following sample figure will show the result of pixel selecting.

Figure 32 shows the original locations of ten samples in the picture. All the samples were randomly chosen.

Figure 32. The original location of each sample

Figure 33 shows the position of sample 1 in the matrix. The red frame indicates the area of sample 1. The frame size of the sample is 11 by 7. As in the principle mentioned above, this area is a continuous number pattern in the matrix. Additionally, the continuous number pattern is surrounded by 0s. The edge of the crack is clearly seen in the image.

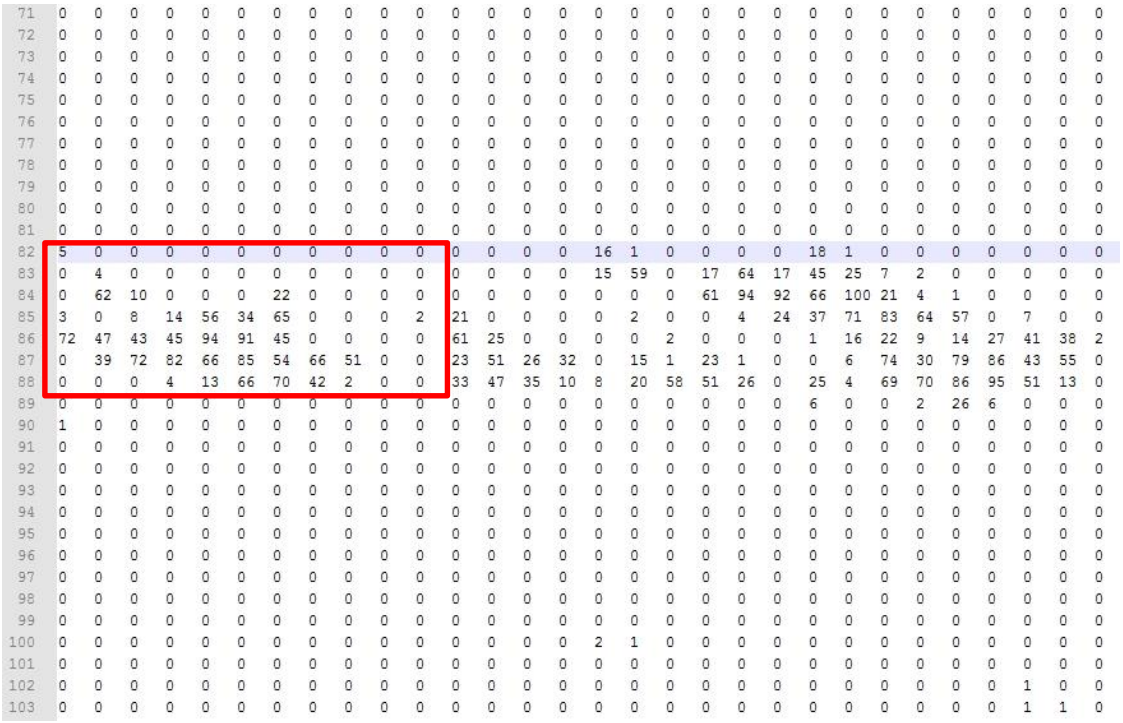

71	0	0	0	0	0	0	0	0	0	0	0	0	0	0	0	0	0	0	0	0	0	0	0	0	0	0	0	0
72	0	0	0	0	0	0	0	0	0	0	0	0	0	0	0	0	0	0	0	0	0	0	0	0	0	0	0	0
73	0	0	0	0	0	0	0	0	0	0	0	0	0	0	0	0	0	0	0	0	0	0	0	0	0	0	0	0
74	0	0	0	0	0	0	0	0	0	0	0	0	0	0	0	0	0	0	0	0	0	0	0	0	0	0	0	0
75	0	0	0	0	0	0	0	0	0	0	0	0	0	0	0	0	0	0	0	0	0	0	0	0	0	0	0	0
76	0	0	0	0	0	0	0	0	0	0	0	0	0	0	0	0	0	0	0	0	0	0	0	0	0	0	0	0
77	0	0	0	0	0	0	0	0	0	0	0	0	0	0	0	0	0	0	0	0	0	0	0	0	0	0	0	0
78	0	0	0	0	0	0	0	0	0	0	0	0	0	0	0	0	0	0	0	0	0	0	0	0	0	0	0	0
79	0	0	0	0	0	0	0	0	0	0	0	0	0	0	0	0	0	0	0	0	0	0	0	0	0	0	0	0
80	0	0	0	0	0	0	0	0	0	0	0	0	0	0	0	0	0	0	0	0	0	0	0	0	0	0	0	0
81	0	0	0	0	0	0	0	0	0	0	0	0	0	0	0	0	0	0	0	0	0	0	0	0	0	0	0	0
82	5	0	0	0	0	0	0	0	0	0	0	0	0	0	0	16	1	0	0	0	0	18	1	0	0	0	0	0
83	0	4	0	0	0	0	0	0	0	0	0	0	0	0	0	15	59	0	17	64	17	45	25	7	2	0	0	0
84	0	62	10	0	0	0	22	0	0	0	0	0	0	0	0	0	0	0	61	94	92	66	100	21	4	1	0	0
85	3	0	8	14	56	34	65	0	0	0	2	21	0	0	0	0	2	0	0	4	24	37	71	83	64	57	0	7
86	72	47	43	45	94	91	45	0	0	0	0	61	25	0	0	0	0	2	0	0	0	1	16	22	9	14	27	41
87	0	39	72	82	66	85	54	66	51	0	0	23	51	26	32	0	15	1	23	1	0	0	6	74	30	79	86	43
88	0	0	0	4	13	66	70	42	2	0	0	33	47	35	10	8	20	58	51	26	0	25	4	69	70	86	95	51
89	0	0	0	0	0	0	0	0	0	0	0	0	0	0	0	0	0	0	0	0	0	6	0	0	2	26	6	0
90	1	0	0	0	0	0	0	0	0	0	0	0	0	0	0	0	0	0	0	0	0	0	0	0	0	0	0	0
91	0	0	0	0	0	0	0	0	0	0	0	0	0	0	0	0	0	0	0	0	0	0	0	0	0	0	0	0
92	0	0	0	0	0	0	0	0	0	0	0	0	0	0	0	0	0	0	0	0	0	0	0	0	0	0	0	0
93	0	0	0	0	0	0	0	0	0	0	0	0	0	0	0	0	0	0	0	0	0	0	0	0	0	0	0	0
94	0	0	0	0	0	0	0	0	0	0	0	0	0	0	0	0	0	0	0	0	0	0	0	0	0	0	0	0
95	0	0	0	0	0	0	0	0	0	0	0	0	0	0	0	0	0	0	0	0	0	0	0	0	0	0	0	0
96	0	0	0	0	0	0	0	0	0	0	0	0	0	0	0	0	0	0	0	0	0	0	0	0	0	0	0	0
97	0	0	0	0	0	0	0	0	0	0	0	0	0	0	0	0	0	0	0	0	0	0	0	0	0	0	0	0
98	0	0	0	0	0	0	0	0	0	0	0	0	0	0	0	0	0	0	0	0	0	0	0	0	0	0	0	0
99	0	0	0	0	0	0	0	0	0	0	0	0	0	0	0	0	0	0	0	0	0	0	0	0	0	0	0	0
100	0	0	0	0	0	0	0	0	0	0	0	0	0	0	0	2	1	0	0	0	0	0	0	0	0	0	0	0
101	0	0	0	0	0	0	0	0	0	0	0	0	0	0	0	0	0	0	0	0	0	0	0	0	0	0	0	0
102	0	0	0	0	0	0	0	0	0	0	0	0	0	0	0	0	0	0	0	0	0	0	0	0	0	0	1	0
103	0	0	0	0	0	0	0	0	0	0	0	0	0	0	0	0	0	0	0	0	0	0	0	0	0	0	1	1

Figure 33. The location of sample 1 in the matrix

Figure 34 shows the position of sample 1 in the original image. In the original image, the color inside the crack is darker than the surrounding area. Thus, the crack could be identified by the naked eye. According to the principle of detecting crack, the color inside the crack is darker than the surrounding areas. This principle of crack detection was performed as continuous number pattern and it is surrounded by 0s in the matrix. Therefore, sample 1 could be accurately defined as a crack after the pixel selecting process.

Figure 34. The location of sample 1 in original image

Figure 35 shows the position of sample 2 in the matrix. The red frame indicates the area of the sample 2, with a frame size of 27 by 33. The continuous number pattern is surrounded by 0s. The edge of the crack is clearly in the image. However, in the middle of Figure 35, there is a number pattern that extends the outline of the continuous number pattern. This kind of pattern will also be defined as a crack by the pixel selecting method.

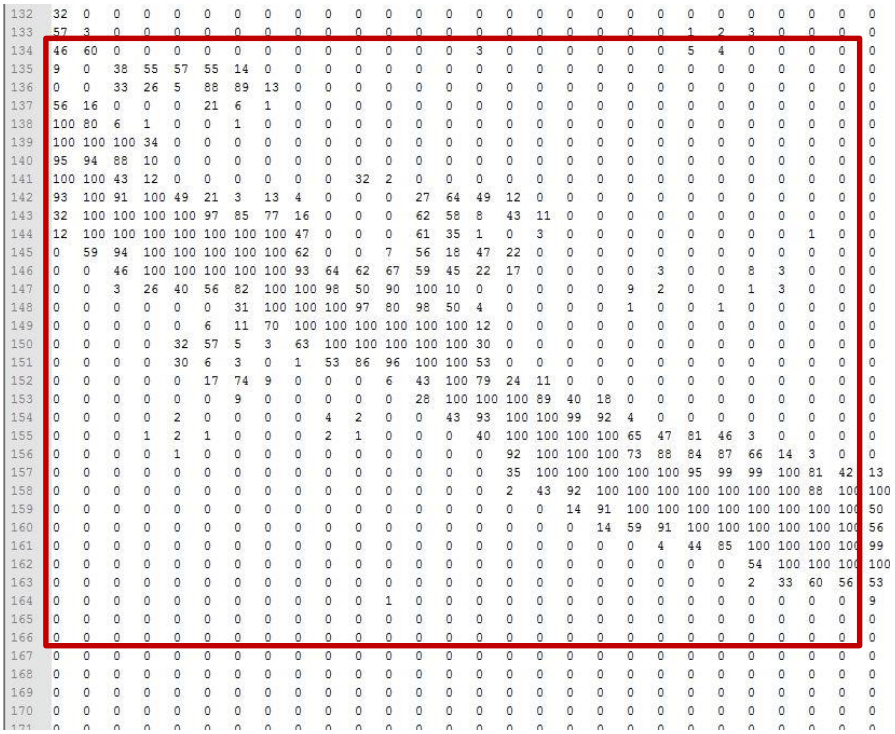

132	32	0	0	0	0	0	0	0	0	0	0	0	0	0	0	0	0	0	0	0	0	0	0	0	0	0
133	57	3	0	0	0	0	0	0	0	0	0	0	0	0	0	0	0	0	0	0	1	2	3	0	0	0
134	46	60	0	0	0	0	0	0	0	0	0	0	0	0	3	0	0	0	0	0	0	5	4	0	0	0
135	9	0	38	55	57	55	14	0	0	0	0	0	0	0	0	0	0	0	0	0	0	0	0	0	0	0
136	0	0	33	26	5	88	89	13	0	0	0	0	0	0	0	0	0	0	0	0	0	0	0	0	0	0
137	56	16	0	0	0	21	6	1	0	0	0	0	0	0	0	0	0	0	0	0	0	0	0	0	0	0
138	100	80	6	1	0	0	1	0	0	0	0	0	0	0	0	0	0	0	0	0	0	0	0	0	0	0
139	100	100	100	34	0	0	0	0	0	0	0	0	0	0	0	0	0	0	0	0	0	0	0	0	0	0
140	95	94	88	10	0	0	0	0	0	0	0	0	0	0	0	0	0	0	0	0	0	0	0	0	0	0
141	100	100	43	12	0	0	0	0	0	0	32	2	0	0	0	0	0	0	0	0	0	0	0	0	0	0
142	93	100	91	100	49	21	3	13	4	0	0	0	27	64	49	12	0	0	0	0	0	0	0	0	0	0
143	32	100	100	100	100	97	85	77	16	0	0	0	62	58	8	43	11	0	0	0	0	0	0	0	0	0
144	12	100	100	100	100	100	100	100	47	0	0	0	61	35	1	0	3	0	0	0	0	0	0	0	1	0
145	0	59	94	100	100	100	100	100	62	0	0	7	56	18	47	22	0	0	0	0	0	0	0	0	0	0
146	0	0	46	100	100	100	100	100	93	64	62	67	59	45	22	17	0	0	0	0	3	0	0	8	3	0
147	0	0	3	26	40	56	82	100	100	98	50	90	100	10	0	0	0	0	0	9	2	0	0	1	3	0
148	0	0	0	0	0	0	31	100	100	100	97	80	98	50	4	0	0	0	0	1	0	0	1	0	0	0
149	0	0	0	0	0	6	11	70	100	100	100	100	100	100	12	0	0	0	0	0	0	0	0	0	0	0
150	0	0	0	0	32	57	5	3	63	100	100	100	100	100	30	0	0	0	0	0	0	0	0	0	0	0
151	0	0	0	0	30	6	3	0	1	53	86	96	100	100	53	0	0	0	0	0	0	0	0	0	0	0
152	0	0	0	0	0	17	74	9	0	0	0	6	43	100	79	24	11	0	0	0	0	0	0	0	0	0
153	0	0	0	0	0	0	9	0	0	0	0	0	28	100	100	100	89	40	18	0	0	0	0	0	0	0
154	0	0	0	0	2	0	0	0	0	4	2	0	0	43	93	100	100	99	92	4	0	0	0	0	0	0
155	0	0	0	1	2	1	0	0	0	2	1	0	0	0	40	100	100	100	100	65	47	81	46	3	0	0
156	0	0	0	0	1	0	0	0	0	0	0	0	0	0	0	92	100	100	100	73	88	84	87	66	14	3
157	0	0	0	0	0	0	0	0	0	0	0	0	0	0	0	35	100	100	100	100	100	95	99	99	100	81
158	0	0	0	0	0	0	0	0	0	0	0	0	0	0	0	2	43	92	100	100	100	100	100	100	100	88
159	0	0	0	0	0	0	0	0	0	0	0	0	0	0	0	0	0	14	91	100	100	100	100	100	100	100
160	0	0	0	0	0	0	0	0	0	0	0	0	0	0	0	0	0	0	14	59	91	100	100	100	100	100
161	0	0	0	0	0	0	0	0	0	0	0	0	0	0	0	0	0	0	0	0	4	44	85	100	100	100
162	0	0	0	0	0	0	0	0	0	0	0	0	0	0	0	0	0	0	0	0	0	0	0	54	100	100
163	0	0	0	0	0	0	0	0	0	0	0	0	0	0	0	0	0	0	0	0	0	0	0	2	33	60
164	0	0	0	0	0	0	0	0	0	0	0	1	0	0	0	0	0	0	0	0	0	0	0	0	0	0
165	0	0	0	0	0	0	0	0	0	0	0	0	0	0	0	0	0	0	0	0	0	0	0	0	0	0
166	0	0	0	0	0	0	0	0	0	0	0	0	0	0	0	0	0	0	0	0	0	0	0	0	0	0
167	0	0	0	0	0	0	0	0	0	0	0	0	0	0	0	0	0	0	0	0	0	0	0	0	0	0
168	0	0	0	0	0	0	0	0	0	0	0	0	0	0	0	0	0	0	0	0	0	0	0	0	0	0
169	0	0	0	0	0	0	0	0	0	0	0	0	0	0	0	0	0	0	0	0	0	0	0	0	0	0
170	0	0	0	0	0	0	0	0	0	0	0	0	0	0	0	0	0	0	0	0	0	0	0	0	0	0

Figure 35. The location of sample 2 in the matrix

Figure 36 shows the position of sample 2 in the original image. In the original image, the color inside the crack is darker than the surrounding area. Thus, the crack can be identified by the naked eye. According to the principle of detecting cracks, the color inside the crack is darker than the surrounding areas. This principle of crack detection is performed as a continuous number pattern and is surrounded by 0s in the matrix. Therefore, sample 2 is accurately defined as a crack after the pixel selecting process.

Figure 36. The location of sample 2 in the original image

Figure 37 shows the position of sample 3 in the matrix. The red frame indicates the area of the sample 3, with a frame size of 21 by 21. As with the principle mentioned above, this area is a continuous number pattern in the matrix that is surrounded by 0s. The edge of the crack is clearly seen in the image. The outline of this crack is a “T” shape.

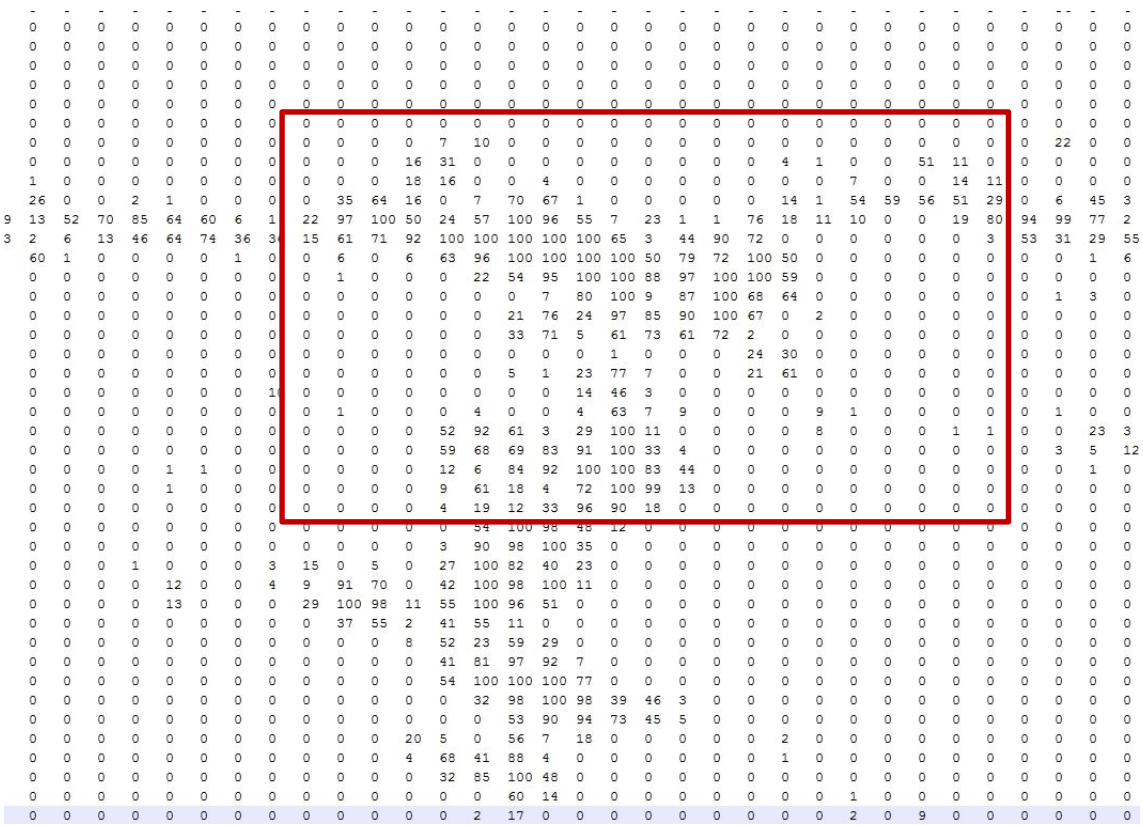

Figure 37. The location of sample 3 in the matrix

Figure 38 shows the position of sample 3 in the original image. In the original image, the color inside the crack is darker than the surrounding area. Thus, the crack can be identified by the naked eye. According to the principles of detecting cracks, the color inside the crack is darker than the surrounding areas. This principle of crack detection is performed as a continuous number pattern and is surrounded by 0s in the matrix. Therefore, sample 3 could be accurately defined as a crack after the pixel selecting process.

Figure 38. The location of sample 3 in the original image

Figure 39 shows the position of sample 4 in the matrix. The red frame indicates the area of the sample 4, with a frame size of 17 by 30. The continuous number pattern is surrounded by 0s. The edge of the crack is clearly seen in the image. There are number patterns outside the outline of the continuous number pattern.

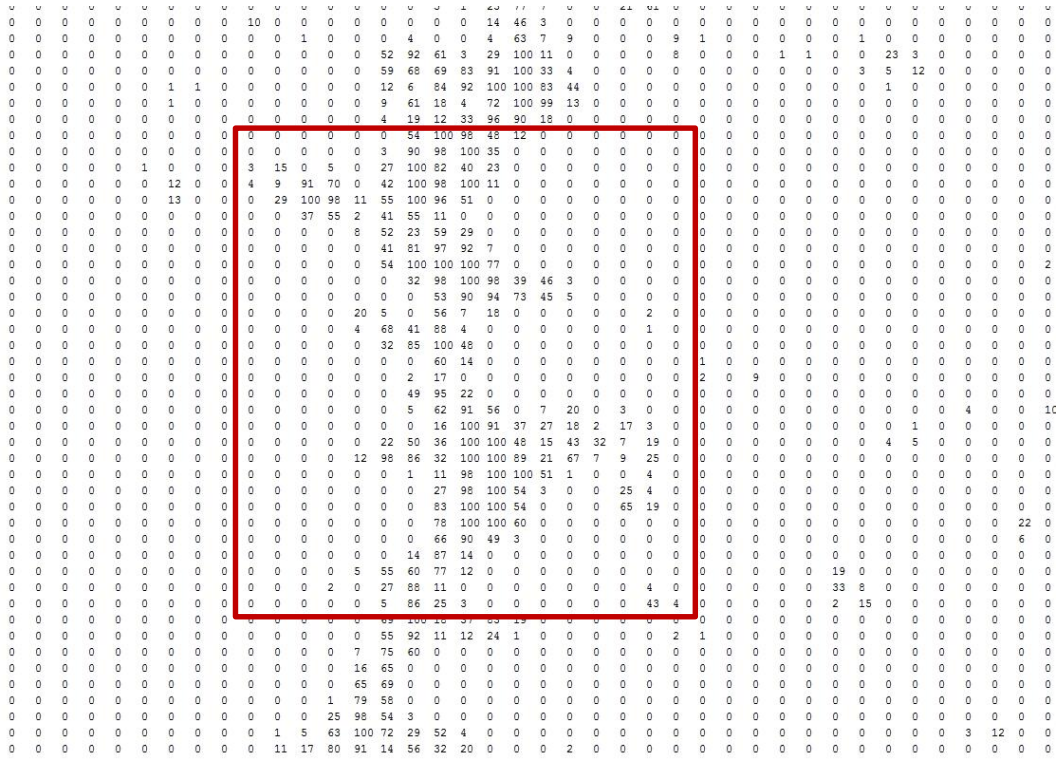

Figure 39. The location of sample 4 in the matrix

Figure 40 shows the position of sample 4 in the original image. In the original image, the color inside the crack is darker than the surrounding area. Thus, the crack can be identified by naked eye. According to the principle of detecting crack, the color inside the crack is darker than the surrounding areas. This principle of crack detection is performed as a continuous number pattern and is surrounded by 0s in the matrix. Therefore, sample 4 is accurately defined as a crack after the pixel selecting process.

Figure 40. The location of sample 4 in the original image

Figure 41 shows the position of sample 5 in the matrix. The red frame indicates the area of the sample 5, with a frame size of 24 by 22. Based on the principle mentioned above, this area is a continuous number pattern in the matrix. Additionally, the continuous number pattern is surrounded by 0s. The edge of the crack can be clearly seen in the image.

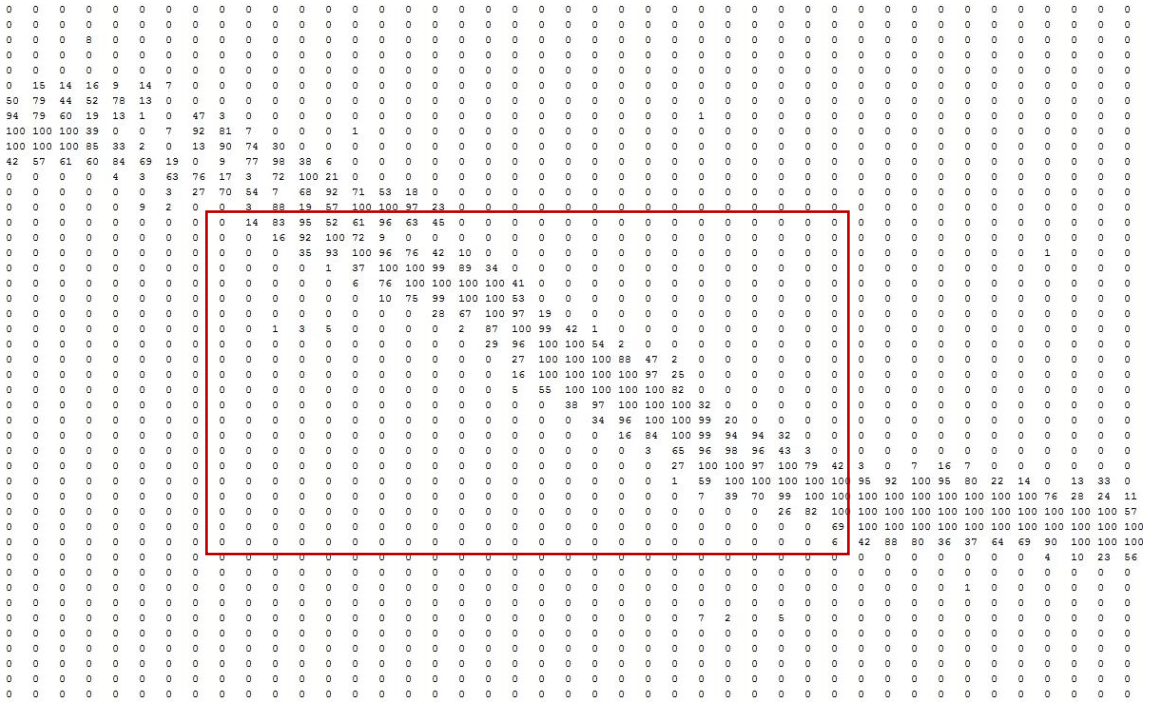

Figure 41. The location of sample 5 in the matrix

Figure 42 shows the position of sample 5 in the original image. In the original image, the color inside the crack is darker than the surrounding area. Thus, the crack can be identified by the naked eye. According to the principle of detecting cracks, the color inside the crack is darker than the surrounding areas. This principle of crack detection is performed as a continuous number pattern and is surrounded by 0s in the matrix. Therefore, sample 5 can be accurately defined as a crack after the pixel selecting process.

Figure 42. The location of sample 5 in the original image

Figure 43 shows the position of sample 6 in the matrix. The red frame indicates the area of the sample 6, with a frame size of 26 by 31. The continuous number pattern is surrounded by 0s. The edge of the crack can be clearly in the image. There are number patterns outside the outline of the continuous number pattern.

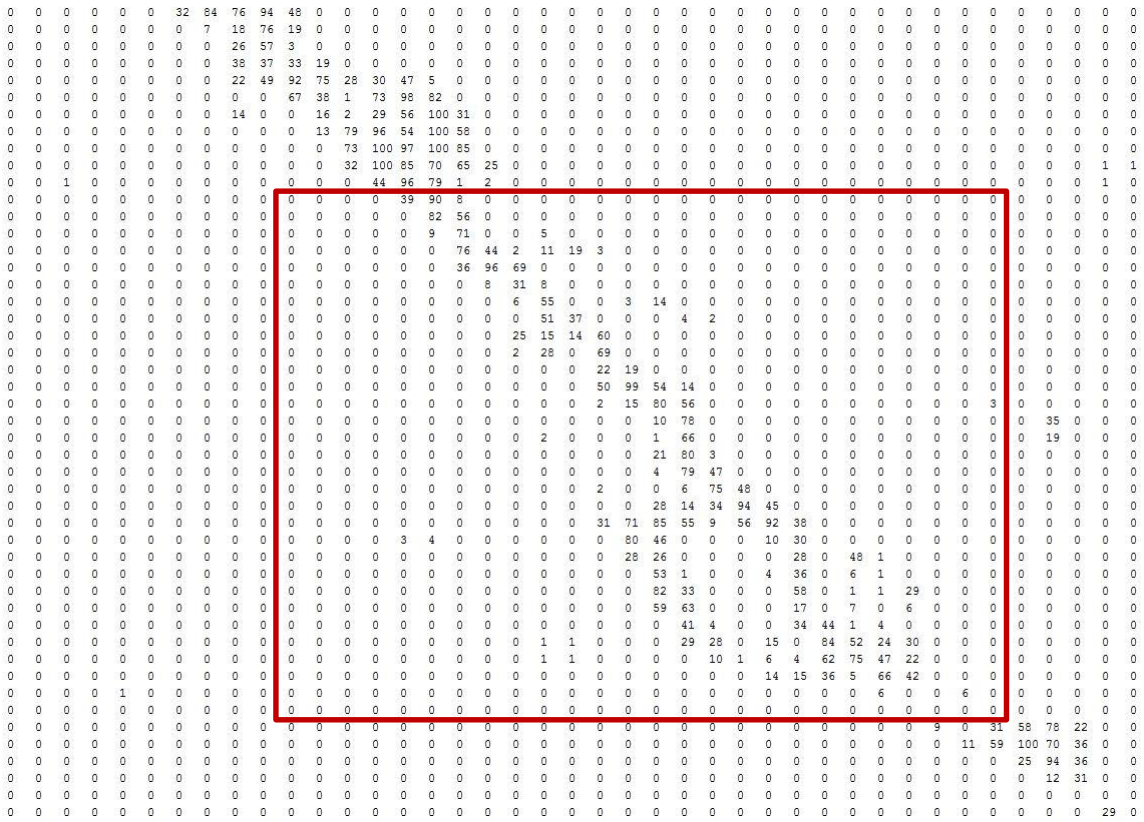

Figure 43. The location of sample 6 in the matrix

Figure 44 shows the position of sample 6 in the original image. In the original image, the color inside the crack is darker than the surrounding area. Thus, the crack can be identified by the naked eye. According to the principle of detecting cracks, the color inside the crack is darker than the surrounding areas. This principle of crack detection is performed as a continuous number pattern and is surrounded by 0s in the matrix. Therefore, sample 6 can be accurately defined as a crack after the pixel selecting process.

Figure 44. The location of sample 6 in the original image

Figure 45 shows the position of sample 7 in the matrix. The red frame indicates the area of sample 7, with a frame size of 13 by 13. Based on the principle mentioned above, this area is a continuous number pattern in the matrix. Additionally, the continuous number pattern is surrounded by 0s. The edge of the crack can be clearly seen in the image.

Figure 45. The location of sample 7 in the matrix

Figure 46 shows the position of sample 7 in the original image. In the original image, the color inside the crack is darker than the surrounding area. Thus, the crack can be identified by the naked eye. According to the principle of detecting cracks, the color inside a crack is darker than the surrounding areas. This principle of crack detection is performed as a continuous number pattern and is surrounded by 0s in the matrix. Therefore, sample 7 can be accurately defined as a crack after the pixel selecting process.

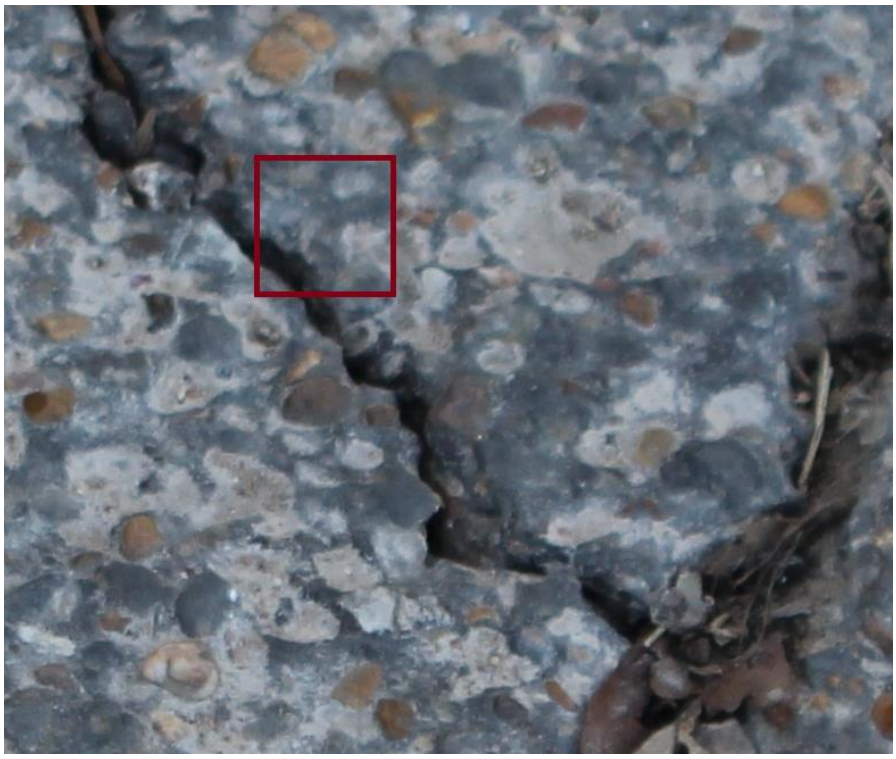

Figure 46. The location of sample 7 in the original image

Figure 47 shows the position of sample 8 in the matrix. The red frame indicates the area of sample 8, with a frame size of 19 by 22. The continuous number pattern is surrounded by 0s. The edge of the crack can be clearly in the image. There are number patterns outside the outline of continuous number pattern.

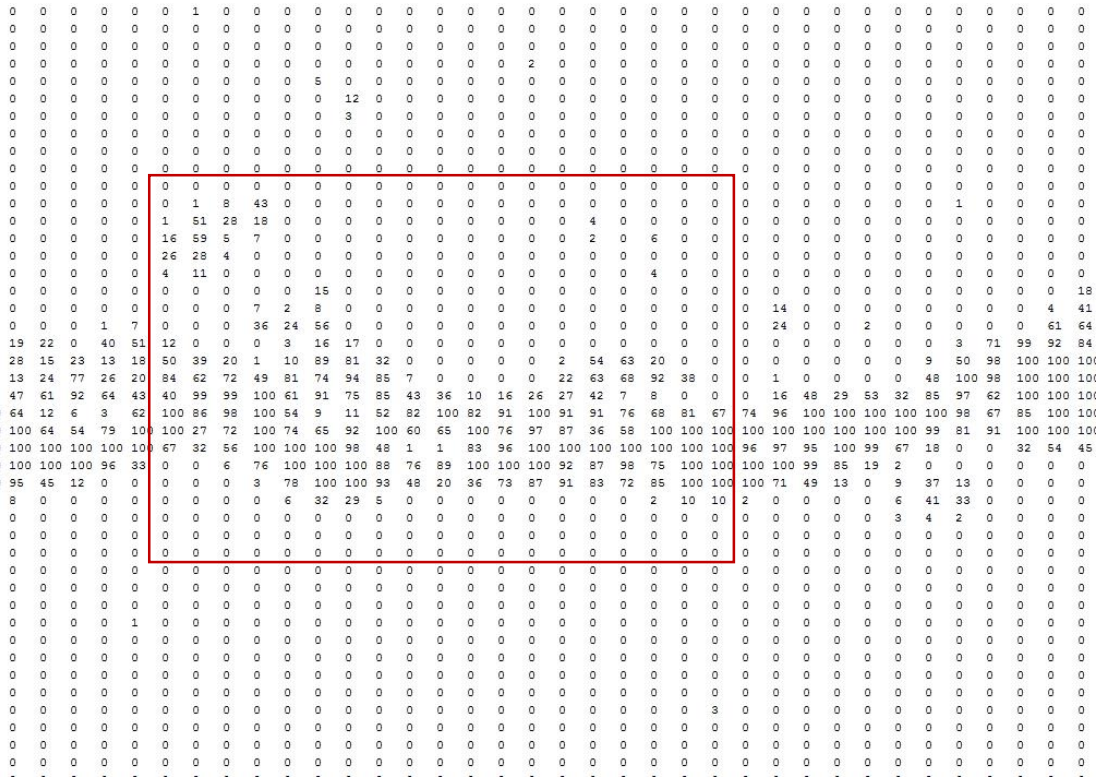

Figure 47. The location of sample 8 in the matrix

Figure 48 shows the position of sample 8 in the original image. In the original image, the color inside the crack is darker than the surrounding area. Thus, the crack can be identified by the naked eye. According to the principle of detecting cracks, the color inside a crack is darker than the surrounding areas. This principle of crack detection is performed as a continuous number pattern and is surrounded by 0s in the matrix. Therefore, sample 8 can be accurately defined as a crack after the pixel selecting process.

Figure 48. The location of sample 8 in the original image

Figure 49 shows the position of sample 9 in the matrix. The red frame indicates the area of sample 9, with a frame size of 17 by 22. Based on the principle mentioned above, this area is a continuous number pattern in the matrix. Additionally, the continuous number pattern is surrounded by 0s. The edge of the crack can be clearly seen in the image.

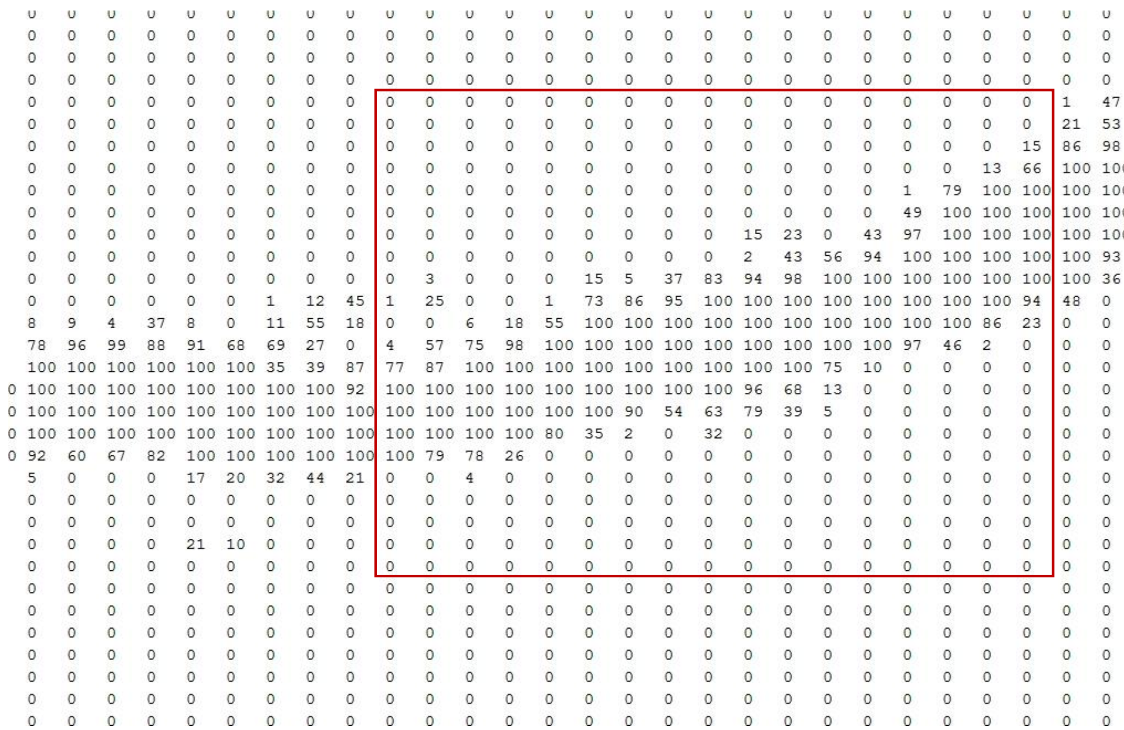

	0	0	0	0	0	0	0	0	0	0	0	0	0	0	0	0	0	0	0	0	0	0	0	0	0	0	0	0
	0	0	0	0	0	0	0	0	0	0	0	0	0	0	0	0	0	0	0	0	0	0	0	0	0	0	0	0
	0	0	0	0	0	0	0	0	0	0	0	0	0	0	0	0	0	0	0	0	0	0	0	0	0	0	0	0
	0	0	0	0	0	0	0	0	0	0	0	0	0	0	0	0	0	0	0	0	0	0	0	0	0	0	0	0
	0	0	0	0	0	0	0	0	0	0	0	0	0	0	0	0	0	0	0	0	0	0	0	0	0	0	1	47
	0	0	0	0	0	0	0	0	0	0	0	0	0	0	0	0	0	0	0	0	0	0	0	0	0	0	21	53
	0	0	0	0	0	0	0	0	0	0	0	0	0	0	0	0	0	0	0	0	0	0	0	0	0	15	86	98
	0	0	0	0	0	0	0	0	0	0	0	0	0	0	0	0	0	0	0	0	0	0	0	0	13	66	100	100
	0	0	0	0	0	0	0	0	0	0	0	0	0	0	0	0	0	0	0	0	0	0	1	79	100	100	100	100
	0	0	0	0	0	0	0	0	0	0	0	0	0	0	0	0	0	0	0	0	0	0	49	100	100	100	100	100
	0	0	0	0	0	0	0	0	0	0	0	0	0	0	0	0	0	0	15	23	0	43	97	100	100	100	100	100
	0	0	0	0	0	0	0	0	0	0	0	0	0	0	0	0	0	0	2	43	56	94	100	100	100	100	100	93
	0	0	0	0	0	0	0	0	0	0	3	0	0	0	15	5	37	83	94	98	100	100	100	100	100	100	100	36
	0	0	0	0	0	0	1	12	45	1	25	0	0	1	73	86	95	100	100	100	100	100	100	100	100	94	48	0
	8	9	4	37	8	0	11	55	18	0	0	6	18	55	100	100	100	100	100	100	100	100	100	100	86	23	0	0
	78	96	99	88	91	68	69	27	0	4	57	75	98	100	100	100	100	100	100	100	100	100	97	46	2	0	0	0
	100	100	100	100	100	100	35	39	87	77	87	100	100	100	100	100	100	100	100	100	75	10	0	0	0	0	0	0
0	100	100	100	100	100	100	100	100	92	100	100	100	100	100	100	100	100	100	96	68	13	0	0	0	0	0	0	0
0	100	100	100	100	100	100	100	100	100	100	100	100	100	100	100	90	54	63	79	39	5	0	0	0	0	0	0	0
0	100	100	100	100	100	100	100	100	100	100	100	100	100	80	35	2	0	32	0	0	0	0	0	0	0	0	0	0
0	92	60	67	82	100	100	100	100	100	100	79	78	26	0	0	0	0	0	0	0	0	0	0	0	0	0	0	0
	5	0	0	0	17	20	32	44	21	0	0	4	0	0	0	0	0	0	0	0	0	0	0	0	0	0	0	0
	0	0	0	0	0	0	0	0	0	0	0	0	0	0	0	0	0	0	0	0	0	0	0	0	0	0	0	0
	0	0	0	0	0	0	0	0	0	0	0	0	0	0	0	0	0	0	0	0	0	0	0	0	0	0	0	0
	0	0	0	0	21	10	0	0	0	0	0	0	0	0	0	0	0	0	0	0	0	0	0	0	0	0	0	0
	0	0	0	0	0	0	0	0	0	0	0	0	0	0	0	0	0	0	0	0	0	0	0	0	0	0	0	0
	0	0	0	0	0	0	0	0	0	0	0	0	0	0	0	0	0	0	0	0	0	0	0	0	0	0	0	0
	0	0	0	0	0	0	0	0	0	0	0	0	0	0	0	0	0	0	0	0	0	0	0	0	0	0	0	0
	0	0	0	0	0	0	0	0	0	0	0	0	0	0	0	0	0	0	0	0	0	0	0	0	0	0	0	0
	0	0	0	0	0	0	0	0	0	0	0	0	0	0	0	0	0	0	0	0	0	0	0	0	0	0	0	0
	0	0	0	0	0	0	0	0	0	0	0	0	0	0	0	0	0	0	0	0	0	0	0	0	0	0	0	0
	0	0	0	0	0	0	0	0	0	0	0	0	0	0	0	0	0	0	0	0	0	0	0	0	0	0	0	0
	0	0	0	0	0	0	0	0	0	0	0	0	0	0	0	0	0	0	0	0	0	0	0	0	0	0	0	0

Figure 49. The location of sample 9 in the matrix

Figure 50 shows the position of sample 9 in the original image. In the original image, the color inside the crack is darker than the surrounding area. Thus, the crack can be identified by the naked eye. According to the principle of detecting cracks, the color inside a crack is darker than the surrounding areas. This principle of crack detection is performed as a continuous number pattern and is surrounded by 0s in the matrix. Therefore, sample 9 can be accurately defined as a crack after the pixel selecting process.

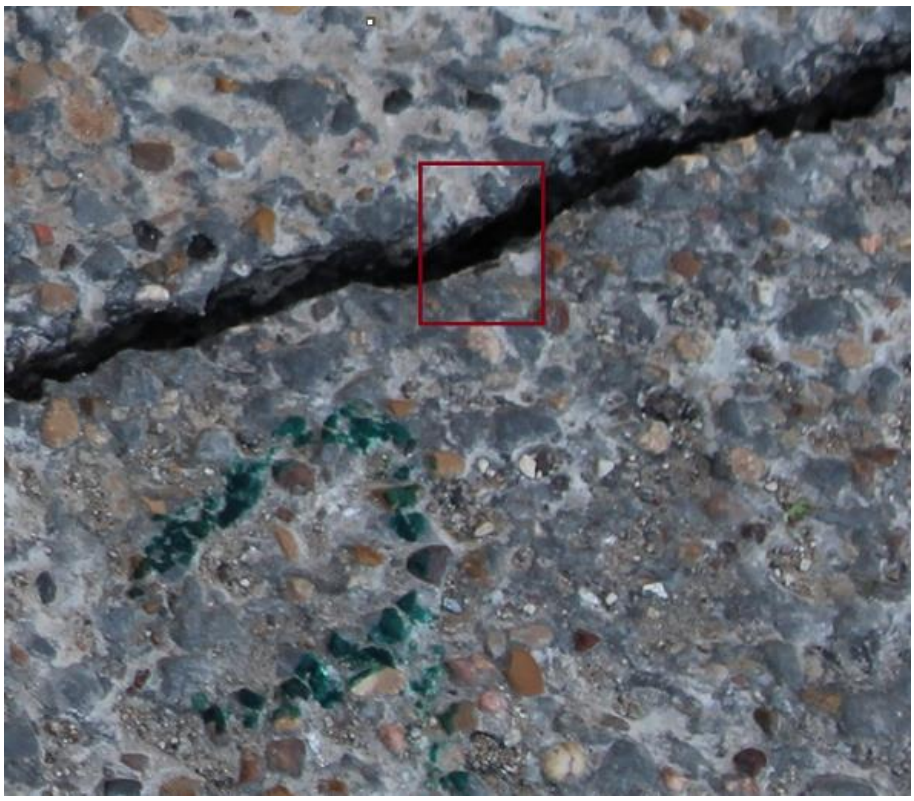

Figure 50. The location of sample 9 in the original image

Figure 51 shows the position of sample 10 in the matrix. The red frame indicates the area of sample 10, with a frame size of 11 by 19. The continuous number pattern is surrounded by 0. The edge of the crack can be clearly in the image. There are number patterns outside the outline of the continuous number pattern.

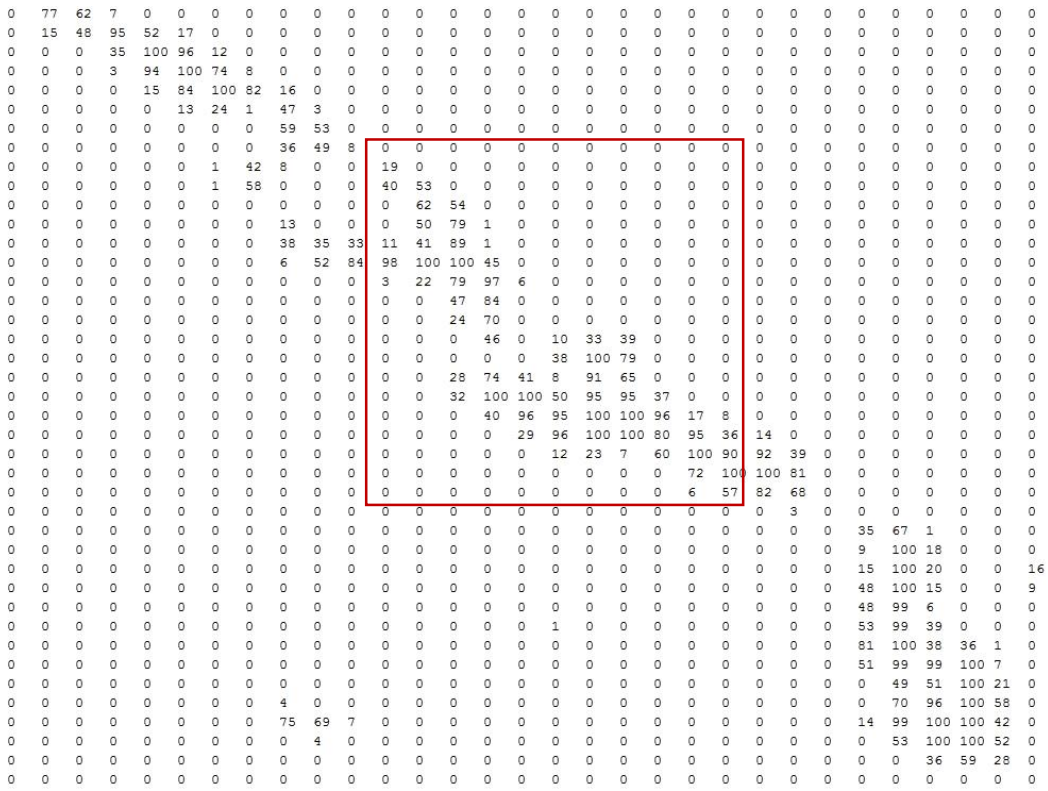

0	77	62	7	0	0	0	0	0	0	0	0	0	0	0	0	0	0	0	0	0	0	0	0	0	0	0	0	0	0
0	15	48	95	52	17	0	0	0	0	0	0	0	0	0	0	0	0	0	0	0	0	0	0	0	0	0	0	0	0
0	0	0	35	100	96	12	0	0	0	0	0	0	0	0	0	0	0	0	0	0	0	0	0	0	0	0	0	0	0
0	0	0	3	94	100	74	8	0	0	0	0	0	0	0	0	0	0	0	0	0	0	0	0	0	0	0	0	0	0
0	0	0	0	15	84	100	82	16	0	0	0	0	0	0	0	0	0	0	0	0	0	0	0	0	0	0	0	0	0
0	0	0	0	0	13	24	1	47	3	0	0	0	0	0	0	0	0	0	0	0	0	0	0	0	0	0	0	0	0
0	0	0	0	0	0	0	0	59	53	0	0	0	0	0	0	0	0	0	0	0	0	0	0	0	0	0	0	0	0
0	0	0	0	0	0	0	0	36	49	8	0	0	0	0	0	0	0	0	0	0	0	0	0	0	0	0	0	0	0
0	0	0	0	0	0	1	42	8	0	0	19	0	0	0	0	0	0	0	0	0	0	0	0	0	0	0	0	0	0
0	0	0	0	0	0	1	58	0	0	0	40	53	0	0	0	0	0	0	0	0	0	0	0	0	0	0	0	0	0
0	0	0	0	0	0	0	0	0	0	0	0	62	54	0	0	0	0	0	0	0	0	0	0	0	0	0	0	0	0
0	0	0	0	0	0	0	0	13	0	0	0	50	79	1	0	0	0	0	0	0	0	0	0	0	0	0	0	0	0
0	0	0	0	0	0	0	0	38	35	33	11	41	89	1	0	0	0	0	0	0	0	0	0	0	0	0	0	0	0
0	0	0	0	0	0	0	0	6	52	84	98	100	100	45	0	0	0	0	0	0	0	0	0	0	0	0	0	0	0
0	0	0	0	0	0	0	0	0	0	0	3	22	79	97	6	0	0	0	0	0	0	0	0	0	0	0	0	0	0
0	0	0	0	0	0	0	0	0	0	0	0	0	47	84	0	0	0	0	0	0	0	0	0	0	0	0	0	0	0
0	0	0	0	0	0	0	0	0	0	0	0	0	24	70	0	0	0	0	0	0	0	0	0	0	0	0	0	0	0
0	0	0	0	0	0	0	0	0	0	0	0	0	0	46	0	10	33	39	0	0	0	0	0	0	0	0	0	0	0
0	0	0	0	0	0	0	0	0	0	0	0	0	0	0	38	100	79	0	0	0	0	0	0	0	0	0	0	0	0
0	0	0	0	0	0	0	0	0	0	0	0	0	28	74	41	8	91	65	0	0	0	0	0	0	0	0	0	0	0
0	0	0	0	0	0	0	0	0	0	0	0	0	32	100	100	50	95	95	37	0	0	0	0	0	0	0	0	0	0
0	0	0	0	0	0	0	0	0	0	0	0	0	0	40	96	95	100	100	96	17	8	0	0	0	0	0	0	0	0
0	0	0	0	0	0	0	0	0	0	0	0	0	0	0	29	96	100	100	80	95	36	14	0	0	0	0	0	0	0
0	0	0	0	0	0	0	0	0	0	0	0	0	0	0	0	12	23	7	60	100	90	92	39	0	0	0	0	0	0
0	0	0	0	0	0	0	0	0	0	0	0	0	0	0	0	0	0	0	0	72	100	100	81	0	0	0	0	0	0
0	0	0	0	0	0	0	0	0	0	0	0	0	0	0	0	0	0	0	0	6	57	82	68	0	0	0	0	0	0
0	0	0	0	0	0	0	0	0	0	0	0	0	0	0	0	0	0	0	0	0	0	0	3	0	0	0	0	0	0
0	0	0	0	0	0	0	0	0	0	0	0	0	0	0	0	0	0	0	0	0	0	0	0	0	35	67	1	0	0
0	0	0	0	0	0	0	0	0	0	0	0	0	0	0	0	0	0	0	0	0	0	0	0	0	9	100	18	0	0
0	0	0	0	0	0	0	0	0	0	0	0	0	0	0	0	0	0	0	0	0	0	0	0	0	15	100	20	0	0
0	0	0	0	0	0	0	0	0	0	0	0	0	0	0	0	0	0	0	0	0	0	0	0	0	48	100	15	0	0
0	0	0	0	0	0	0	0	0	0	0	0	0	0	0	0	0	0	0	0	0	0	0	0	0	48	99	6	0	0
0	0	0	0	0	0	0	0	0	0	0	0	0	0	0	0	1	0	0	0	0	0	0	0	0	53	99	39	0	0
0	0	0	0	0	0	0	0	0	0	0	0	0	0	0	0	0	0	0	0	0	0	0	0	0	81	100	38	36	1
0	0	0	0	0	0	0	0	0	0	0	0	0	0	0	0	0	0	0	0	0	0	0	0	0	51	99	99	100	7
0	0	0	0	0	0	0	0	0	0	0	0	0	0	0	0	0	0	0	0	0	0	0	0	0	0	49	51	100	21
0	0	0	0	0	0	0	0	4	0	0	0	0	0	0	0	0	0	0	0	0	0	0	0	0	0	70	96	100	58
0	0	0	0	0	0	0	0	75	69	7	0	0	0	0	0	0	0	0	0	0	0	0	0	0	14	99	100	100	42
0	0	0	0	0	0	0	0	0	4	0	0	0	0	0	0	0	0	0	0	0	0	0	0	0	0	53	100	100	52
0	0	0	0	0	0	0	0	0	0	0	0	0	0	0	0	0	0	0	0	0	0	0	0	0	0	0	36	59	28
0	0	0	0	0	0	0	0	0	0	0	0	0	0	0	0	0	0	0	0	0	0	0	0	0	0	0	0	0	0

Figure 51. The location of sample 10 in the matrix

Figure 52 shows the position of sample 10 in the original image. In the original image, the color inside the crack is darker than the surrounding area. Thus, the crack can be identified by the naked eye. According to the principle of detecting cracks, the color inside a crack is darker than the surrounding areas. This principle of crack detection is performed as a continuous number pattern and is surrounded by 0s in the matrix. Therefore, sample 10 can be accurately defined as a crack after the pixel selecting process.

Figure 52. The location of sample 10 in the original image

Based on the 10 sample results above, continuous number patterns surrounded by 0s are defined as cracks during the pixel selecting phase. The edges of cracks can be accurately detected and the influence points or pattern are also removed by the pixel selecting method. Based on the original images, the cracks which are detected in the matrix can be shown to be the cracks in the original images.

STATISTICAL ANALYSIS

The statistical analysis is the final process for the crack detection model. The purpose of this process is to prove that the linear regression line of a continuous number pattern is the center line for the actual crack. Based on the results from the pixel selecting process, the continuous number patterns in the matrix were proved to be the actual cracks in the original images. However, these conclusions are based on the results of edge detection. Additional results based on statistical analysis are still needed. Therefore, the statistical analysis is the final process for the crack detection model. The following paragraph will introduce the process of statistical analysis.

As mentioned above, the general idea of the crack detection model is to transform the photogrammetric data into statistical data. Compared to other crack detection methods, the crack detection model uses a statistical method to detect cracks. In this study, each sample will be transformed into an X and Y coordinate. As mentioned in the pixel selecting process, the continuous number lines surrounded by 0s have been detected as the actual cracks in the original images. Therefore, the numbers in the matrix which are not 0 are the objects for statistical analysis.

In other words, each number in this X and Y coordinate will only be defined as "exist" or "not exist." If the number in the coordinate is 0, it will be ignored in this study. If the number of the coordinate is not 0, it will be defined as an object in the statistical analysis. The coordinates which are not 0 will be analyzed using SAS statistical software. The linear regression lines will be the center lines of the cracks in the original pictures. The linear regression line was diagnosed by the P-value, R-square and residuals. In the pixel selection process, the edge of the crack was detected. In this process, the linear regression line will be proven to be the center line for the crack. Using the linear regression line as the center line for the crack, the crack can be outlined by using this statistical method. Figure 53 shows the general picture of crack detection. The crack in the figure is a small crack similar to the samples in this study. Therefore, this crack detection model can identify the cracks in this study.

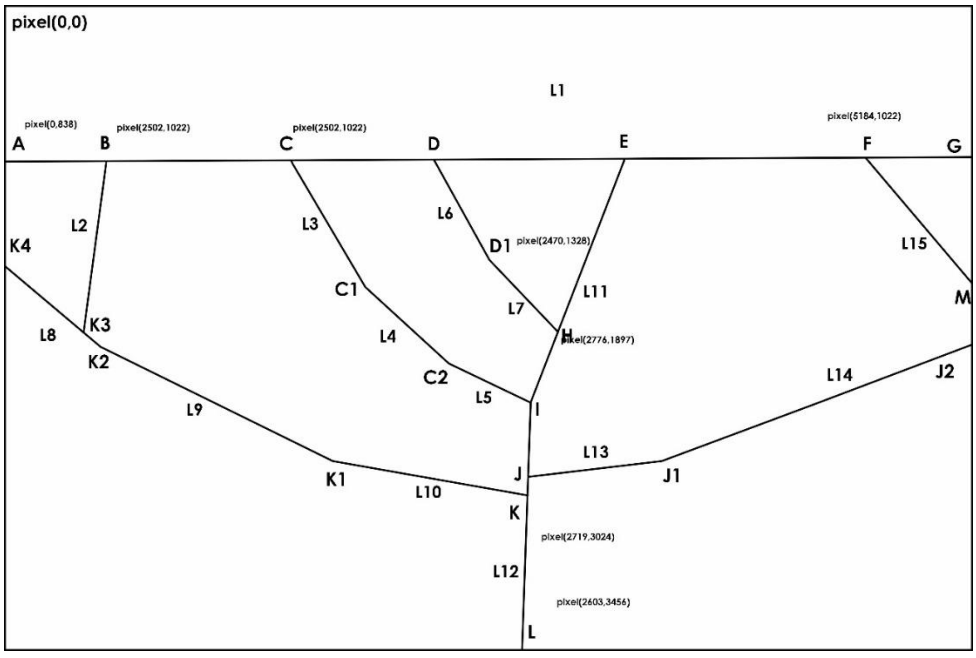

Figure 53. The draft result of crack detection for crack No.3

CHAPTER IV

RESULTS

INTRODUCTION

This chapter summarizes the results of the samples mentioned above. The statistical analysis focuses on non-zero coordinates in the matrix. The linear regression lines were analyzed by the P-value, R-square and residuals. The linear regression line was proven to be the center line for the crack. At the same time, because of the thesis limitations in this study, some cracks could not be detected by this method, such as sample 3 the “T” shaped crack. Therefore, in future studies, the research should focus on how to detect cracks that are not linear segments.

THE RESULT OF SAMPLE 2

The results for sample 2 will be presented in this paragraph. The linear regression line for sample 2 is proved to be the center line for the actual crack. Figure 36 shows sample 2 in the original picture. In Figure 35, sample 2 starts at (0,134) to (27,166) in the new matrix. The block size of the second selection is 10 x 10. The original matrix in the first selection should be 10 times larger than the new matrix. Therefore, the coordinates in the original picture of sample 2 should be (0, 1340) to (270, 1660). The original location of sample 2 can be easily identified in the original image.

Furthermore, the matrix of sample 2 was transformed into Microsoft Excel. Figure 54 shows the X and Y coordinates in Microsoft Excel. In the statistical analysis process, the numbers in each box do not refer to the weight of the pixels. If the number is 0, it

will be ignored in this analysis. If the number is not 0, it will be treated as an object for the statistical process. For instance, coordinate (1, 1) will be treated as an object in the statistical process and coordinate (1, 3) will be ignored.

For the linear regression, no zero coordinates were analyzed by SAS. The linear regression line is the straight line shown in Figure 55. Figure 55 also indicates that most of the points are located inside the 95% prediction limits. The R-square of the regression line is 0.5291. The strength of the regression is accepted in this study. In Figure 56, the data are randomly located around 0 which means that there is constant variance for the data. Most of all, Figure 57 shows the P-value of the data is smaller than 0.0001, which proves that the data can be represented by linear regression. At the same time, the residual and percent figure indicates that the data in each row are distributed as a normal distribution. It also means that the data fit the linear regression. Therefore, the regression line of the data is proved as a linear regression line. Figure 56 also proves that the distance from linear regression to the edge of the crack is equal, based on constant variance. Therefore, the linear regression line of the continuous number patterns is the center line for the actual crack in the original image.

Figure 54 shows the matrix of sample 2. A continuous number pattern line can be easily identified in the figure. The coordinates which are 0 were ignored in this study. No zero coordinates were analyzed by the regression model.

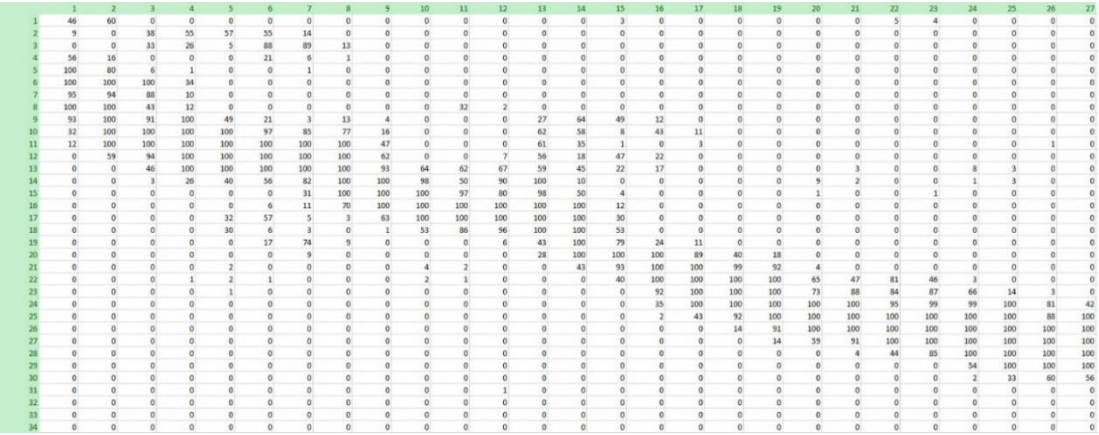

	1	2	3	4	5	6	7	8	9	10	11	12	13	14	15	16	17	18	19	20	21	22	23	24	25	26	27
1	46	60	0	0	0	0	0	0	0	0	0	0	0	0	3	0	0	0	0	0	0	5	4	0	0	0	0
2	9	0	38	55	57	55	14	0	0	0	0	0	0	0	0	0	0	0	0	0	0	0	0	0	0	0	0
3	0	0	33	26	5	88	89	13	0	0	0	0	0	0	0	0	0	0	0	0	0	0	0	0	0	0	0
4	56	16	0	0	0	21	6	1	0	0	0	0	0	0	0	0	0	0	0	0	0	0	0	0	0	0	0
5	100	80	6	1	0	0	1	0	0	0	0	0	0	0	0	0	0	0	0	0	0	0	0	0	0	0	0
6	100	100	100	34	0	0	0	0	0	0	0	0	0	0	0	0	0	0	0	0	0	0	0	0	0	0	0
7	95	94	88	10	0	0	0	0	0	0	0	0	0	0	0	0	0	0	0	0	0	0	0	0	0	0	0
8	100	100	43	12	0	0	0	0	0	0	32	2	0	0	0	0	0	0	0	0	0	0	0	0	0	0	0
9	93	100	91	100	49	21	3	13	4	0	0	0	27	64	49	12	0	0	0	0	0	0	0	0	0	0	0
10	32	100	100	100	100	97	85	77	16	0	0	0	62	58	8	43	11	0	0	0	0	0	0	0	0	0	0
11	12	100	100	100	100	100	100	100	47	0	0	0	61	35	1	0	3	0	0	0	0	0	0	0	0	1	0
12	0	59	94	100	100	100	100	100	62	0	0	7	56	18	47	22	0	0	0	0	0	0	0	0	0	0	0
13	0	0	46	100	100	100	100	100	93	64	62	67	59	45	22	17	0	0	0	0	3	0	0	8	3	0	0
14	0	0	3	26	40	56	82	100	100	98	50	90	100	10	0	0	0	0	0	9	2	0	0	1	3	0	0
15	0	0	0	0	0	0	31	100	100	100	97	80	98	50	4	0	0	0	0	1	0	0	1	0	0	0	0
16	0	0	0	0	0	6	11	70	100	100	100	100	100	100	12	0	0	0	0	0	0	0	0	0	0	0	0
17	0	0	0	0	32	57	5	3	63	100	100	100	100	100	30	0	0	0	0	0	0	0	0	0	0	0	0
18	0	0	0	0	30	6	3	0	1	53	86	96	100	100	53	0	0	0	0	0	0	0	0	0	0	0	0
19	0	0	0	0	0	17	74	9	0	0	0	6	43	100	79	24	11	0	0	0	0	0	0	0	0	0	0
20	0	0	0	0	0	0	9	0	0	0	0	0	28	100	100	100	89	40	18	0	0	0	0	0	0	0	0
21	0	0	0	0	2	0	0	0	0	4	2	0	0	43	93	100	100	99	92	4	0	0	0	0	0	0	0
22	0	0	0	1	2	1	0	0	0	2	1	0	0	0	40	100	100	100	100	65	47	81	46	1	0	0	0
23	0	0	0	0	1	0	0	0	0	0	0	0	0	0	0	92	100	100	100	73	88	84	87	66	14	3	0
24	0	0	0	0	0	0	0	0	0	0	0	0	0	0	0	35	100	100	100	100	100	95	99	99	100	81	42
25	0	0	0	0	0	0	0	0	0	0	0	0	0	0	0	2	43	92	100	100	100	100	100	100	100	88	100
26	0	0	0	0	0	0	0	0	0	0	0	0	0	0	0	0	0	14	91	100	100	100	100	100	100	100	100
27	0	0	0	0	0	0	0	0	0	0	0	0	0	0	0	0	0	0	14	59	91	100	100	100	100	100	100
28	0	0	0	0	0	0	0	0	0	0	0	0	0	0	0	0	0	0	0	0	4	44	85	100	100	100	100
29	0	0	0	0	0	0	0	0	0	0	0	0	0	0	0	0	0	0	0	0	0	0	0	54	100	100	100
30	0	0	0	0	0	0	0	0	0	0	0	0	0	0	0	0	0	0	0	0	0	0	0	2	33	60	56
31	0	0	0	0	0	0	0	0	0	0	0	1	0	0	0	0	0	0	0	0	0	0	0	0	0	0	0
32	0	0	0	0	0	0	0	0	0	0	0	0	0	0	0	0	0	0	0	0	0	0	0	0	0	0	0
33	0	0	0	0	0	0	0	0	0	0	0	0	0	0	0	0	0	0	0	0	0	0	0	0	0	0	0
34	0	0	0	0	0	0	0	0	0	0	0	0	0	0	0	0	0	0	0	0	0	0	0	0	0	0	0

Figure 54. The result of sample 2 in Microsoft Excel

Figure 55 shows the plot of the data in sample 2. There are 281 observations in this analysis. Most of the data are located inside the 95% prediction limits.

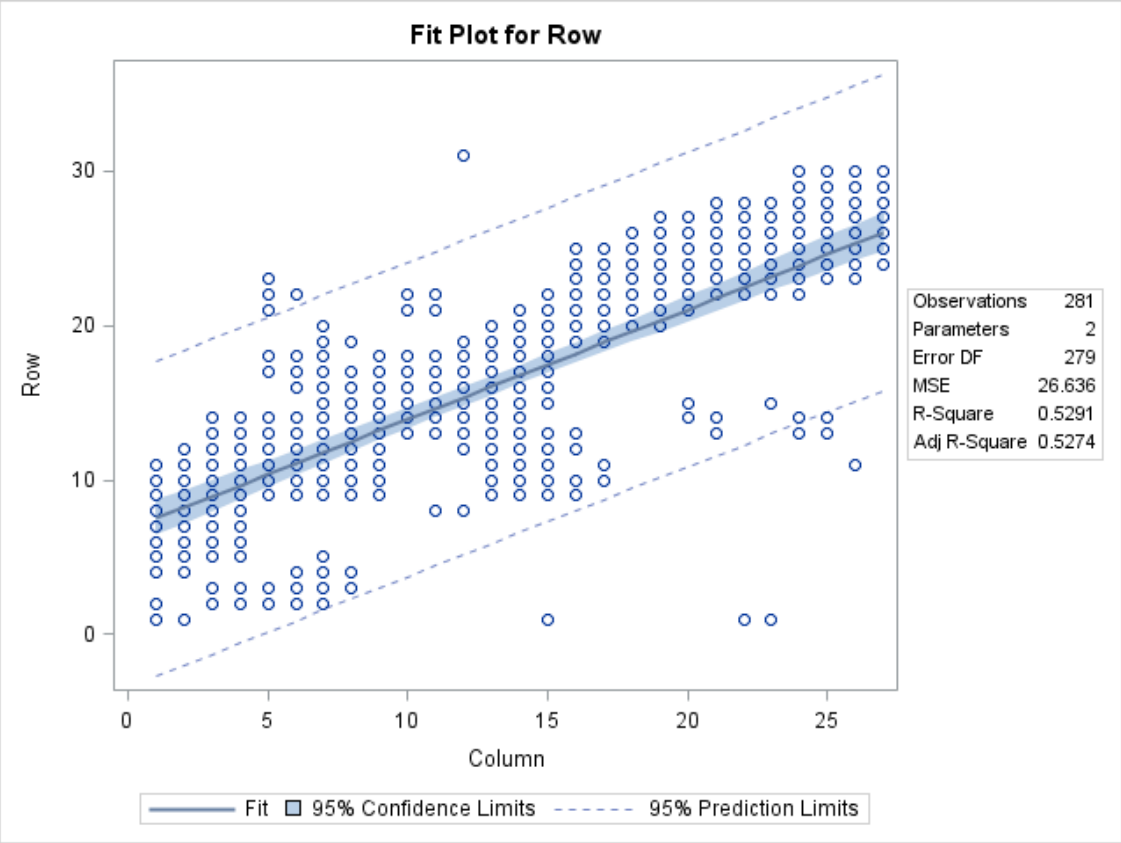

Figure 55. The plot of the linear regression

Figure 56 shows the result of residuals in sample 2. In this figure, all the data are randomly located around 0. This means there is a constant variance in the linear regression model.

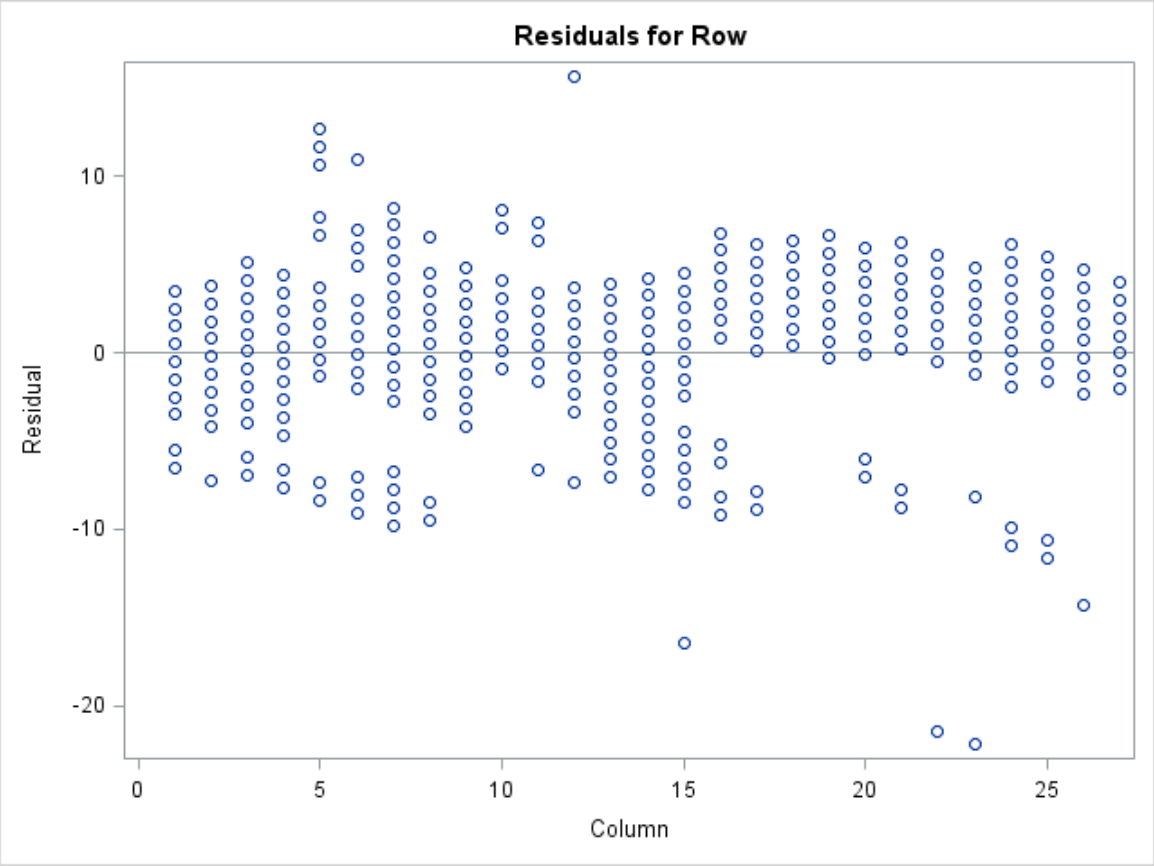

Figure 56. The result of residuals

Figure 57 shows the result of analysis of variance. In this figure, the P-value is smaller than 0.0001 which means that the line was proven to be a linear regression line.

The SAS System

The REG Procedure
Model: MODEL1
Dependent Variable: Row

Number of Observations Read	281
Number of Observations Used	281

Analysis of Variance

Source	DF	Sum of Squares	Mean Square	F Value	Pr > F
Model	1	8350.39237	8350.39237	313.50	<.0001
Error	279	7431.40834	26.63587		
Corrected Total	280	15782			

Root MSE	5.16100	R-Square	0.5291
Dependent Mean	16.17082	Adj R-Sq	0.5274
Coeff Var	31.91549		

Parameter Estimates

Variable	DF	Parameter Estimate	Standard Error	t Value	Pr > |t|
Intercept	1	6.79219	0.61266	11.09	<.0001
Column	1	0.71265	0.04025	17.71	<.0001

Figure 57. Results of the analysis of variance

Figure 58 shows the fit diagnostics for the data. In the picture of percent and residual, the data in each row is distributed as a normal distribution.

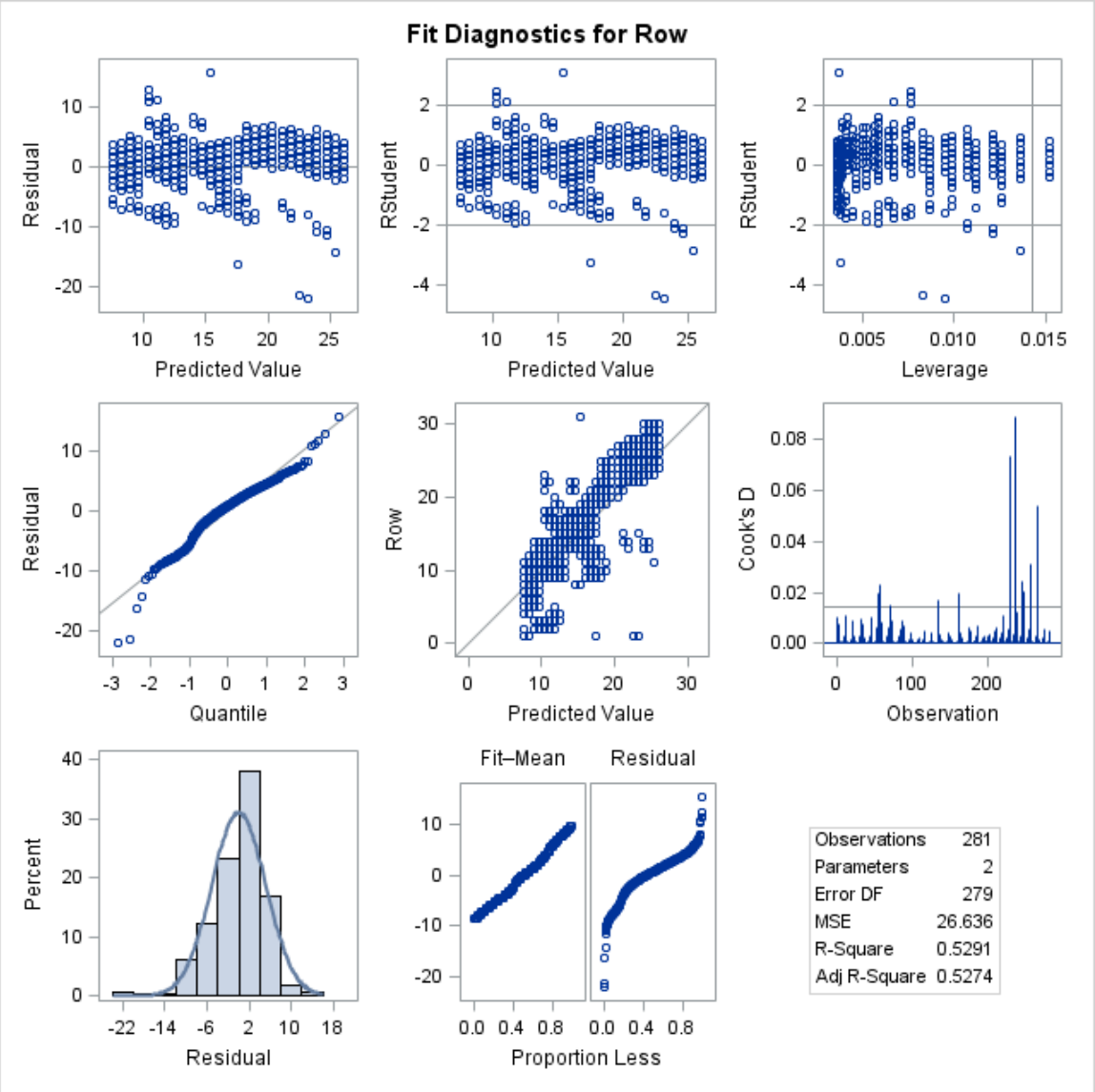

Figure 58. Fit diagnostics for Row

THE STUDY LIMITATION OF SAMPLE 3

This study has some limitations. Some cracks could not be identified by this method; for example, the “T” shaped crack in sample 3 could not be analyzed. This kind of crack could not be defined as a linear regression line. This problem must be solved in future research.

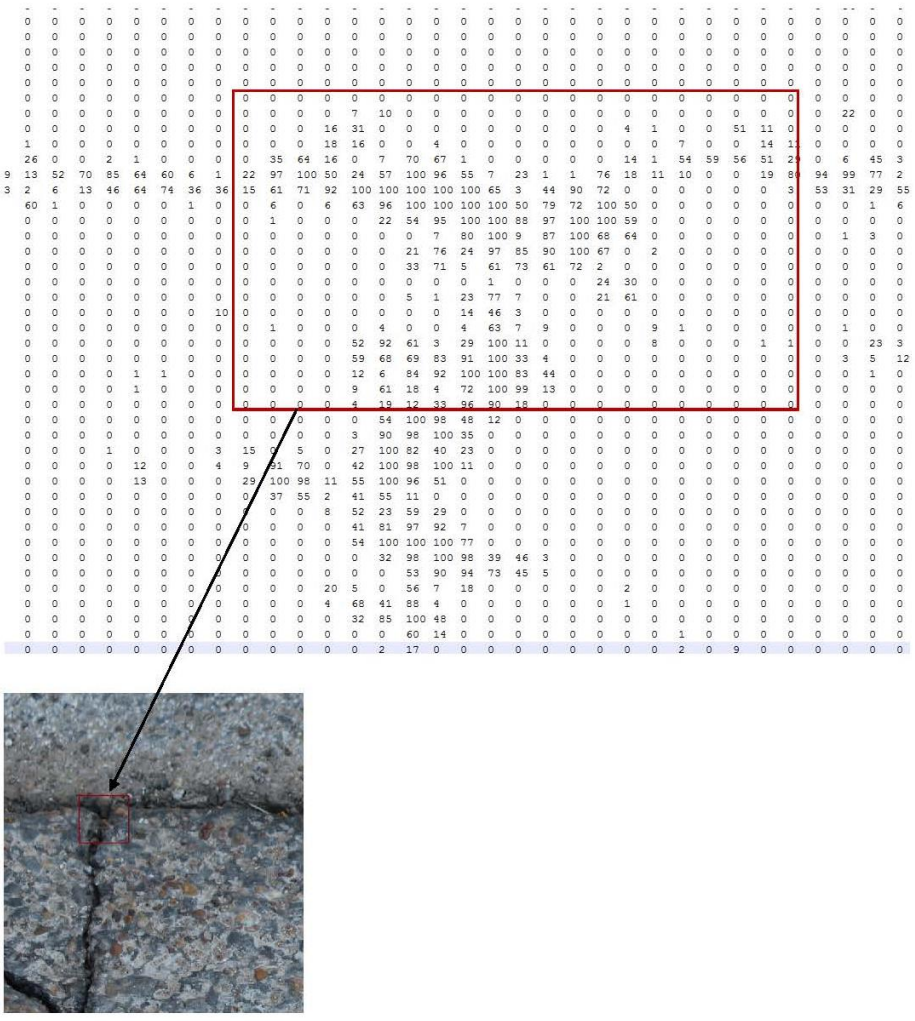

Figure 59. The crack which could not be solved by this method

CHAPTER V

CONCLUSION

This research study uses a crack detection model to identify cracks on a road. The crack detection model is an important process in a Visual Pattern Recognition (VPR) model. There are four components in the crack detection model: image collection, image segmentation, pixel selection and statistical analysis. This study starts with image collection to collect the pictures of cracks on the road. Then, image segmentation was used to transform the original image into a binary image. In this process, the images were converted into 0 and 1 matrices. The R (Red) value was treated as primary threshold in this phase. Subsequently, the pixel selecting phase was used to sum up the pixels in the matrix and resize the matrix. Finally, the resized matrix was statistically analyzed using linear regression. The linear regression line was treated as the center line of the crack in the original image.

The hypothesis one mentioned above that all pixels can be accurately selected by the R (Red) value in the image segmentation phase. Different R values will be used in the RGB (Red Green Blue) selecting algorithm. The R thresholding value which is 50 seems to be a suitable R value in this study. The outline of the crack could be clearly shown and there are few influence points or patterns in the binary image. Therefore, the R thresholding value could be used in the future study.

The hypothesis two mentioned above that the block can accurately count the pixel number. The edge of the crack can be accurately defined by the pixel selection and the

continuous pixel pattern will be treated as a crack. From the result of the tem samples in pixel selection phase, the pixel selection method could accurately remove the noise in binary image and define the edge of the crack.

From the result of sample 2, the regression line was shown to represent a theoretical center line of the actual crack. However, some cracks could not be detected by using this method. This kind of crack, such as sample 3, the "T" shaped crack, cannot be detected using this model. Therefore, future research should focus on:

- Finding an efficient way to identify cracks that are not a linear line;
- Developing an accurate selecting R value in the image segmentation phase;
- Developing a suitable block size in the pixel selection phase; and
- Developing a more efficient pixel selecting algorithm to remove the influence points and patterns in the binary images.

REFERENCES

Abdel-Qader, I., Abudayyeh, O., & Kelly, M. E. (2003). Analysis of edge-detection techniques for crack identification in bridges. *Journal of Computing in Civil Engineering*, *17*(4), 255-263.

Adu-Gyamfi, Y., Okine, N. A., Garateguy, G., Carrillo, R., & Arce, G. R. (2011). Multiresolution information mining for pavement crack image analysis. *Journal of Computing in Civil Engineering*, *26*(6), 741-749.

Brilakis, I., German, S., & Zhu, Z. (2011). Visual pattern recognition models for remote sensing of civil infrastructure. *Journal of Computing in Civil Engineering*, *25*(5), 388-393.

Deason, J. P. (1998). Toward improved highway quality: Lessons from western europe. *Journal of Management in Engineering*, *14*(1), 81-86.

Goedert, J., Bonsell, J., & Samura, F. (2005). Integrating laser scanning and rapid prototyping to enhance construction modeling. *Journal of Architectural Engineering*, *11*(2), 71-74.

Hwang, H., & Haddad, R. (1995). Adaptive median filters: New algorithms and results. *Image Processing, IEEE Transactions on*, *4*(4), 499-502.

Jog, G., Koch, C., Golparvar-Fard, M., & Brilakis, I. (2012). Pothole properties measurement through visual 2D recognition and 3D reconstruction. Paper presented at the *Computing in Civil Engineering (2012),* pp. 553-560.

Koch, C., & Brilakis, I. (2011). Pothole detection in asphalt pavement images. *Advanced Engineering Informatics, 25*(3), 507-515.

Koch, C., Jog, G. M., & Brilakis, I. (2012). Automated pothole distress assessment using asphalt pavement video data. *Journal of Computing in Civil Engineering, 27*(4), 370-378.

Li, L., Sun, L., Tan, S., & Ning, G. (2014). An efficient way in image preprocessing for pavement crack images. *Bridges, 10*, 9780784412442.315.

Liang, S., & Sun, B. (2010). Using wavelet technology for pavement crack detection. Paper presented at the *ICLEM 2010@ sLogistics for Sustained Economic Development: Infrastructure, Information, Integration,* pp. 2479-2484.

Maode, Y., Shaobo, B., Kun, X., & Yuyao, H. (2007). Pavement crack detection and analysis for high-grade highway. Paper presented at the *Electronic Measurement and Instruments, 2007. ICEMI'07. 8th International Conference on,* pp. 4-548-4-552.

Memon, Z. A., Majid, M. Z. A., & Mustaffar, M. (2005). An automatic project progress monitoring model by integrating AutoCAD and digital photos. Paper presented at the *Proc. of the ASCE International Conference on Computing in Civil Engineering,*

Mikhail, E. M., Bethel, J. S., & McGlone, J. C. (2001). *Introduction to modern photogrammetry* John Wiley & Sons Inc.

Parker, J. R. (2010). *Algorithms for image processing and computer vision* John Wiley & Sons.

Torok, M. M., Golparvar-Fard, M., & Kochersberger, K. B. (2013). Image-based automated 3D crack detection for post-disaster building assessment. *Journal of Computing in Civil Engineering,*

Wang, S., Wu, E., Liu, Y., Liu, X., & Chen, Y. (2012). Abstract line drawings from photographs using flow-based filters. *Computers & Graphics, 36*(4), 224-231.o

Wang, Z., & Zhang, D. (1999). Progressive switching median filter for the removal of impulse noise from highly corrupted images. *Circuits and Systems II: Analog and Digital Signal Processing, IEEE Transactions on, 46*(1), 78-80.

FYu, X., Li, Y., & Wu, J. (2011). Study on maintenance quality evaluation system of arterial highway asphalt pavement. Paper presented at the *11th International Conference of Chinese Transportation Professionals (ICCTP),*

Zack, G. W., Rogers, W. E., & Latt, S. A. (1977). Automatic measurement of sister chromatid exchange frequency. *The Journal of Histochemistry and Cytochemistry : Official Journal of the Histochemistry Society, 25*(7), 741-753.

Zou, Q., Cao, Y., Li, Q., Mao, Q., & Wang, S. (2012). CrackTree: Automatic crack detection from pavement images. *Pattern Recognition Letters, 33*(3), 227-238.

APPENDIX

Table 1. The programing code of MATLAB in the image segmentation process

```
im = imread('IMG_3019.JPG');
figure, imshow(im)
im_R = im(:,:,1);
figure, imshow(im_R)
im_R_10 = im_R < 10;
figure, imshow(im_R_10 * 255);
figure, imshow(im)
figure, imshow((1-im_R_10) * 255
im_R_150 = im_R < 150;
result = (1-im_R_150) * 255;
figure, imshow(result);
imwrite(result, 'out_150.bmp');
```

Table 2. The program code of MATLAB in pixel selecting process

```
image=imread('out_50.bmp');
%???????1????0
image(image==0)=1;
image(image>1)=0;

%????????
[le,wi]=size(image);
block_size=10;%????????
ln=fix(le/block_size);
wn=fix(wi/block_size);
lrem=rem(le,block_size);
wrem=rem(wi,block_size);
vectorl=linspace(block_size,block_size,ln);
vectorw=linspace(block_size,block_size,wn);
vectorl=[vectorl lrem];
vectorw=[vectorw wrem];
c=mat2cell(image,vectorl,vectorw);

%???????
result=zeros(length(vectorl),length(vectorw));
for i=1:1:length(vectorl)
    for j=1:1:length(vectorw)
        a=cell2mat(c(i,j));
        result(i,j)=sum(a(:));
    end
end
%??excel
fid=fopen('result.txt','wt');
[m,n]=size(result);
for i=1:1:m
    for j=1:1:n
        if j==n
            fprintf(fid,'%g\n',result(i,j));
        else
            fprintf(fid,'%g\t',result(i,j));
        end
    end
end
fclose(fid);
```